MOLECULAR LUMINESCENCE SPECTROMETRY WITH AN ELECTRIC DISCHARGE UNDER REDUCED PRESSURE

BY

TIING YU

A DISSERTATION PRESENTED TO THE GRADUATE SCHOOL
OF THE UNIVERSITY OF FLORIDA IN
PARTIAL FULFILLMENT OF THE REQUIREMENTS
FOR THE DEGREE OF DOCTOR OF PHILOSOPHY

UNIVERSITY OF FLORIDA

1987

Dedicated to my dearest parents and wife

ACKNOWLEDGEMENTS

I would like to express my deepest gratitude to Dr. James D. Winefordner for his guidance, patience and support. I have always found encouragement from his incredible optimism and enthusiasm. My thanks go to Drs. John Dorsey, E. Muschlitz and Rick Yost for the invaluable discussions. A special thanks goes to Dr. Yost for his very helpful advice (chemistry as well as English) on writing the dissertation.

I feel so lucky to have had the opportunity to work with such distinguished, outstanding scientists who have extended my knowledge in chemistry. Among them, I would like to mention Drs. Alain Berthod, K. P. Li, Bachoo Patel, Kiyoshi Tanabe, Ben Smith (the great student sitter) and Ray von Wandruszka. Friendship makes life more rewarding and I thank all the JDW group members, especially Leigh Ann Files, Doug Goforth, Audrey Wang, Jose Lanauze, Mario Tremblay and Moi Leung. The help from the glass shop, machine shop and electronics shop has been indispensable and is greatly appreciated. Thanks go to Jeanne Karably for her assistance throughout the years.

I like to say thank you to Jun Liang Lin, a real gentleman. We have been good friends for the last few years. Indeed those few years, we have faced ups and downs together. It has been nice to have a true friend to share these experiences.

TABLE OF CONTENTS

	Page
ACKNOWLEDGEMENTS	iii
ABSTRACT	vi
CHAPTER	
I. INTRODUCTION	1
II. MECHANISM OF EXCITATION PROCESSES IN ELECTRIC DISCHARGES	4
Introduction	4
Literature Review	5
Previous Work	7
Experimental	13
Results	22
$Ar+N_2$ System	23
N_2 System	29
Ar System	30
He System	30
Discussion	31
III. MOLECULAR SPECTRAL ANALYSIS	36
Methods of Analysis	36
Temperature Determination	36
Spectral Measurement of Polycyclic Aromatic Hydrocarbons	39
Molecular spectra	39
Quantitative measurements	40
Experimental	40
The Discharge Tube and Reaction Cell	40
High Voltage Power Supply	45
Detection Systems	47
Chemicals	48
Results and Discussions	48
Excitation Temperatures	48
Discharge Characteristics	50
Spectral Measurements	51
Wavelength calibration	51
Dark current	55
Background radiation	56
Molecular spectra and background compensation method	59
Quantitative measurements	84

CHAPTER Page

IV. CONCLUSIONS AND FUTURE WORK 91

Present Work 91
Future Work 92

REFERENCES 93

BIOGRAPHICAL SKETCH 98

Abstract of Dissertation Presented to the Graduate School of the University of Florida in Partial Fulfillment of the Requirements for the Degree of Doctor of Philosophy

MOLECULAR LUMINESCENCE SPECTROMETRY WITH AN ELECTRIC DISCHARGE UNDER REDUCED PRESSURE

By

Tiing Yu

December, 1987

Chairman : James D. Winefordner
Major Department: Chemistry

A discharge under reduced pressure (0.5-10 torr) created by applying a high voltage (2.0-7.5 kV) alternating current over glass tubes (dielectric material) is described. This research was initiated by the evaluation of the excitation mechanism of benzene and polycyclic aromatic hydrocarbons (PAHs) in the nitrogen afterglow of an electric discharge. The metastable nitrogen molecules $N_2(A)$ were found to be involved in the excitation of mercury and nitric oxide but not benzene and anthracene. The afterglow of helium and argon discharges was also investigated. From the characteristics of the discharge, it was suggested that benzene and PAHs were actually excited in the discharge plasma instead of its afterglow.

The excitation temperatures of argon and helium in the discharge were measured at different applied voltages. The results show the same magnitude within the experimental uncertainty for Ar lines and

He lines. The temperature was very insensitive to changes in the applied voltage. At fixed applied voltage (7.5 kV), the discharge current was measured at different pressures. The current peaked at approximately 1 torr coincident with maximum N_2 emission.

The spectra of twelve compounds were measured with a photodiode array detector. The detection limits for these compounds, evaluated with a single channel detector, were about 1 μg, which is inadequate for trace analysis.

CHAPTER I
INTRODUCTION

For many spectroscopic measurements, excitation sources are needed to pump analyte species from the ground state to an excited state. In the process of flame atomic emission spectrometry (1), kinetic energy is transferred through collisions to excite the analyte. The radiation from a hollow cathode lamp is absorbed by ground state atoms in an atomic absorption measurement (2). In other words, atoms in the ground state are excited by the radiation of the lamp. Xenon arc lamps, mercury lamps and lasers are used as excitation sources in molecular and atomic fluorescence spectroscopies (3,4). Energy released from a chemical reaction can occasionally be employed to pump the reaction products to higher states which can then relax by fluorescence. The determination of nitrogen oxides by the reaction with ozone is one example of this process, called chemiluminescence (5). In addition, many atoms and small molecules can be excited by energy transfer from metastable species (6). Gases such as He, Ar, and N_2 are common metastable energy carriers (6). In an inductively coupled plasma (7) or microwave induced plasma (8), electrons and gaseous metastable atoms and molecules that are created by electron impact are involved in the excitation process. Analytes are broken apart into atoms, ions and radicals which further absorb energy to reach excited states (8). Excitation is also found in many electric discharges (9), such as the

DC arc, AC arc, plasma jet, etc. However, the electric discharge under atmospheric pressure is not the subject of this work.

In this study, an electric discharge at reduced pressure was investigated. Electric discharges under reduced pressure (glow discharges) have long been analytical tools for the determination of atomic species (10-15). However, for the first time, organic molecules have been investigated in this laboratory by electric discharges with concentric glass tubes (16). In a glow discharge, solid samples are analyzed through sputtering (10) which brings the sample molecules from the cathode into the discharge. Liquid samples are dried on the cathode before sputtering begins (17). Gaseous samples are introduced directly into the discharge and therefore the sputtering is not important (18). In our discharge system, a high voltage was applied through a glass tube (dielectric material) to the low pressure space, while in a glow discharge, two metal electrodes are directly inserted into the vacuum space. Samples were introduced into the discharge in the gaseous phase.

This study was actually a continuation of a research project on the subject of "active nitrogen-induced chemiluminescence" that was conducted by former graduate student H. A. Jurgensen in this laboratory (16). Active nitrogen was generated in a glass electrode discharge by applying an alternating current at 2.0-7.5 kV under low pressure (0.5-10 torr) nitrogen flow. Fluorescence of organic molecules, such as naphthalene, was detected in the afterglow of the nitrogen electric discharge. The mechanism of excitation of analytes was proposed as energy transfer through collisions with active

nitrogen metastables - $N_2(A^3\Sigma_u^+)$ (16). In this work, a more detailed investigation was made of the role of $N_2(A^3\Sigma_u^+)$ in the excitation process, and the afterglow of He and Ar was also investigated. From the excitation mechanism study, it was found that the excitation of molecules occurred in the discharge plasma itself instead of in the afterglow region by metastable energy transfer. Therefore, studies on the discharge with the concentric glass tubes were performed which included the diagnostic analysis of the electric discharge system and molecular luminescence measurements of a few polycyclic aromatic hydrocarbons (PAHs) as well as some other hydrocarbons.

CHAPTER II
MECHANISM OF EXCITATION PROCESSES IN ELECTRIC DISCHARGES

Introduction

In the afterglow of an electric discharge produced from flowing nitrogen gas at reduced pressure ~1 torr, many polycyclic aromatic hydrocarbons (PAHs) were excited, and the fluorescence was monitored in previous work in this laboratory (16). Good sensitivity was reported for several PAHs. A mechanism was proposed for the excitation process that considered metastable energy transfer to the sample molecules from so-called "active nitrogen." The long-lived (~2 s) triplet state excited $N_2(A^3\Sigma_u^+)$ molecules were considered as the major species contributing to the reactivity of the active nitrogen. After a close look by the present investigator at these previous experiments, one phenomenon was not clearly explained by this proposed mechanism. Therefore, a study was conducted toward the excitation mechanism of the electric discharge; this was part of an on-going research program on metastable transfer emission spectrometry (MTES) with active nitrogen. The major question yet to be answered was whether the $N_2(A^3\Sigma_u^+)$ molecules were involved in the excitation of large organic molecules. The previous work on the MTES done in this laboratory will be reviewed, followed by a description of the current mechanism investigations.

Literature Review

"Active nitrogen" is usually generated in a flow system by a microwave or electric discharge (19). In analytical studies, analytes are then introduced into the afterglow downstream of the discharge, where only the long-lived metastable molecules exist.

The excitation mechanism of analyte molecules has been considered to involve energy transfer from metastable nitrogen molecules, and thus the name "Metastable Transfer Emission Spectrometry" (MTES). The processes can be expressed as follows:

$$N_2 \xrightarrow{\text{discharge}} N_2^*(M) + N_2^*(E) \qquad (2a)$$

$$N_2^*(M) + A \longrightarrow A^* + N_2 \qquad (2b)$$

$$A^* \longrightarrow A + h\nu \qquad (2c)$$

Metastable states $N_2^*(M)$ and other excited states $N_2^*(E)$ are formed within the microwave or electric discharge. Only metastable $N_2^*(M)$ survives downstream of the flow system to transfer energy by colliding with analyte molecules, A, which are then excited and later relaxed by fluorescence or phosphorescence. Nitrogen A state is the metastable state which has been reported to be involved in the excitation process (19).

The reactions between active nitrogen and various metals, inorganic compounds (such as NO, NO_2, H_2S, etc.), and small organic compounds (such as CH_4, C_2H_2, and C_2H_4) have been extensively studied in the past (19). Analytical applications involving active nitrogen

have drawn considerable attention in the last few years. Using a microwave discharge to generate active nitrogen, Sutton, et al. measured trimethylbismuth and germane (GeH_4) at the ppb level with a linear response over about 5 orders of magnitude (6). Sutton et al. applied the same system to determine Pb with a detection limit of 0.2 ng (6). Fassel et al. (20-23) have measured various atoms and small molecules by using the technique called atmospheric pressure active nitrogen (APAN) spectrometry, where active nitrogen was generated through an electrodeless ozonizer discharge under atmospheric pressure. Na and Niemczyk (24,25) utilized a microwave discharge to generate active nitrogen for the determination of trace metals in aqueous solutions; detection limits for Ag, Bi, Cd, Cu, Mg, Pb and Tl in the low picogram range were reported. They found that matrix interferences with this technique were lower than in electrothermal atomization atomic absorption spectroscopy. Furthermore, they showed that it was possible to do multielement analysis with this technique under proper conditions. Dodge and Allen (26) utilized a high voltage AC electric discharge to generate active nitrogen. Detection limits of 10^8 atoms cm^{-3} and 10^7 cm^{-3} for Hg and Zn were obtained, respectively. Mitchell et al. found an excellent way to determine oxygen-containing impurities in N_2 and Ar gases by monitoring NO γ band radiation (27,28) from the chemiluminescence reaction of oxygen-containing impurities with active nitrogen.

While the measurement of atomic species has been quite successful, only a few molecular species have been investigated by

this technique. Sutton, Westberg and Melzer (29) evaluated a non-selective GC detector for hydrocarbons in which the CN radical formed from the reaction of hydrocarbons with active nitrogen radiated strongly at 383 to 388 nm. The addition of HCl gas to the active nitrogen system was reported to catalyze the production of CN emission. Based on the same mechanism, Rice, et al. (21) applied the APAN technique as a GC detector. Excellent sensitivity and simple instrumentation were cited as advantages for this technique. The development of the active nitrogen technique before 1965 is summarized in the comprehensive book written by Wright and Winkler (19).

Previous Work

In previous research performed in this laboratory (16), the afterglow of N_2 discharge was evaluated as a means of exciting large, highly conjugated molecules, such as PAHs. The detection of PAHs has become an active area of research due to the carcinogenic properties of this class of compounds (30,31). An electric discharge system described by Allen, et al. (26) was applied for this purpose. The discharge cell was constructed of two concentric glass tubes (16), as shown in Figure 1. A high voltage AC (7.5 kV) was applied to the inner tube, which was filled with saturated salt solution; and the outer tube was coated with gold paint, then wrapped with conducting tape and grounded. Benzene and other PAHs were introduced into the afterglow downstream of the discharge cell, with two light traps inserted between the cell and the sample port, as shown in Figure 2. Molecular emission spectra of the intact compounds were obtained

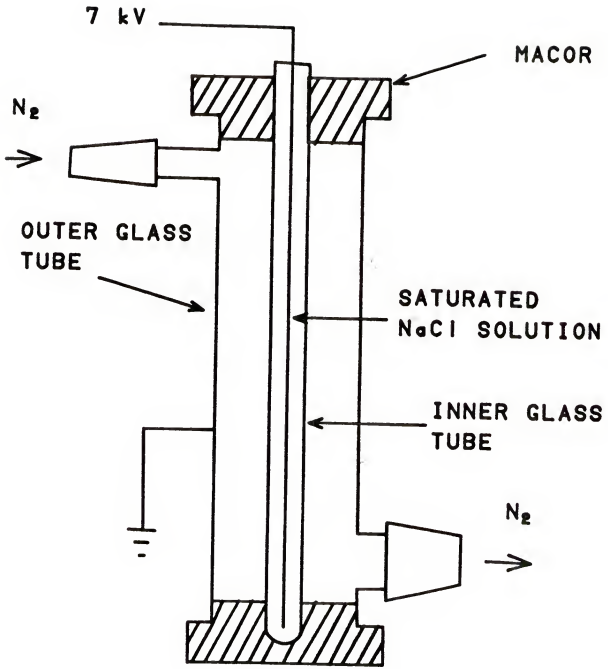

Figure 1
Discharge tube for generation of active nitrogen (16).

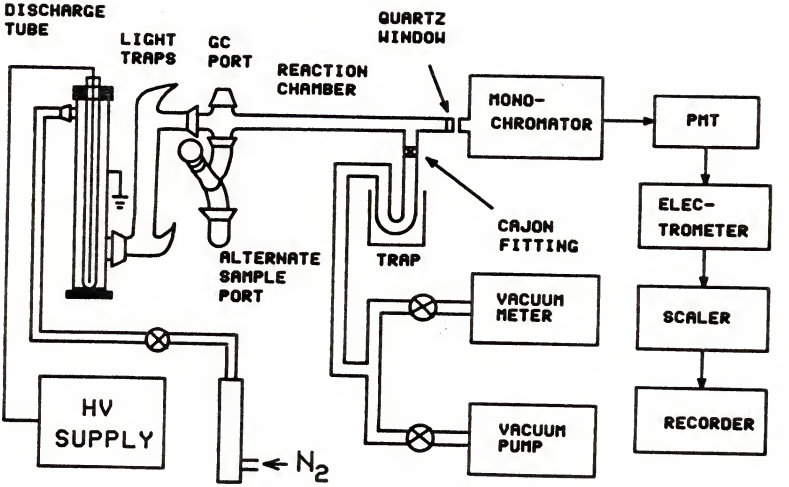

Figure 2
Block diagram of active nitrogen experimental apparatus with sample introduction and detection system (16).

(16), rather than emission spectra of fragments such as CN, C_2, CH, etc. The emission spectrum of benzene is shown in Figure 3 (16). According to these results, $N_2(A)$ seemed to be a reasonable excitation source also for these fluorphores.

However, the dominant background of the N_2 second positive emission (which will be shown later) in the afterglow was not explained. The creation of the $N_2(A)$ has been reported to result from the consecutive decay of excited N_2 from higher excited states (32). The following two steps are responsible for the second positive and first positive radiation, respectively (32) :

$$N_2(C^3\Pi_\mu) \longrightarrow N_2(B^3\Pi_g) + h\nu_2 \text{ (second positive)} \qquad (2d)$$

$$N_2(B^3\Pi_g) \longrightarrow N_2(A^3\Sigma_u^+) + h\nu_1 \text{ (first positive)} \qquad (2e)$$

The partial energy diagram (33) for N_2 is shown in Figure 4. The formation of $N_2(C)$ can be accomplished either by electron impact or the energy pooling reaction of $N_2(A)$ (32), as shown in the following reaction:

$$N2(A^3\Sigma_u^+) + N_2(A^3\Sigma_u^+) \longrightarrow N_2(X^1\Sigma_g^+) + N_2(C^3\Pi_\mu) \qquad (2f)$$

where $N_2(X^1\Sigma_g^+)$ is the nitrogen ground state. It appeared very unlikely that this quantum mechanically forbidden recombination reaction (34) was responsible for the high intensity of the second positive emission. Thus, it was postulated that there could be other energetic species in the reaction cell that populated $N_2(C)$ states

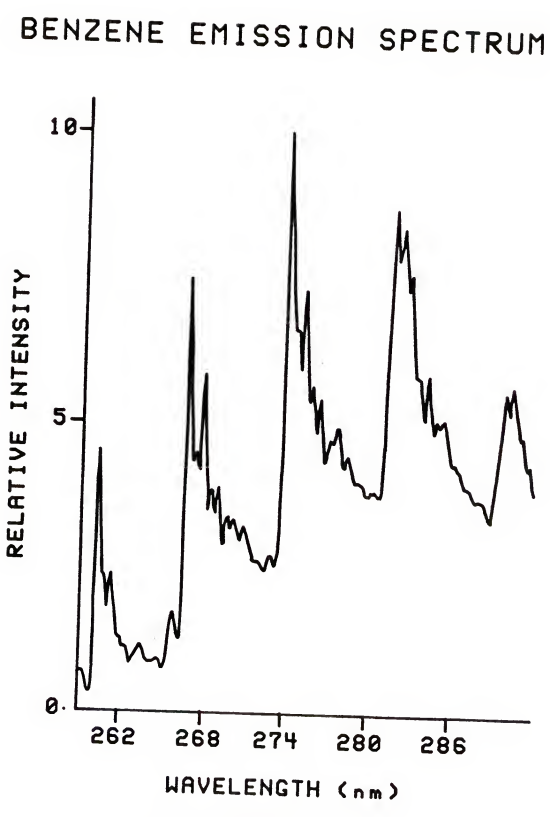

Figure 3
Benzene emission spectrum (16).

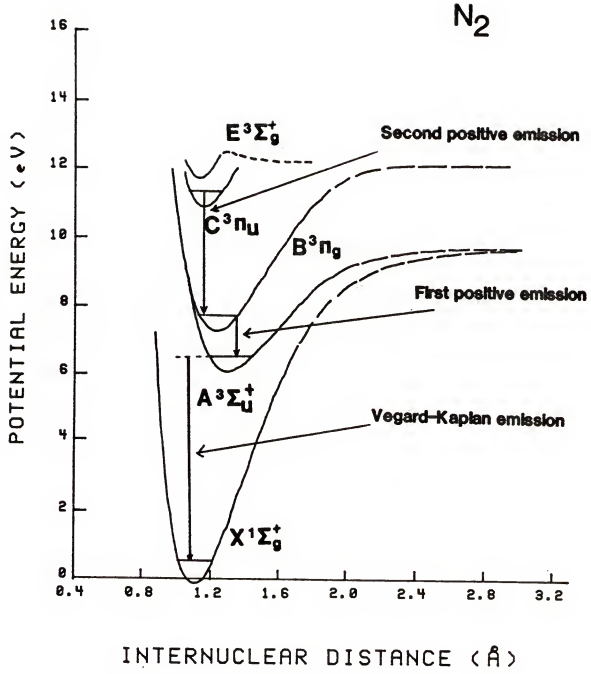

Figure 4
Partial nitrogen energy diagram (33).

and resulted in the intense second positive band. With the presence of many other species in addition to $N_2(A)$ in the reaction cell, the question of whether $N_2(A)$ were the species involved in the excitation of PAHs obviously remained unanswered. Therefore, it was necessary to reevaluate the previously proposed mechanism.

Experimental

A technique developed by Setser, et al. (35-37) was adopted to separate N_2 metastable molecule from other N_2 species in a flowing system. Metastable $N_2(A)$ molecules were generated by the interaction of metastable argon atoms with molecular nitrogen. Through energy transfer, nitrogen molecules were excited to form $N_2(C)$ which later deexcited in two steps, as shown in Equation 2d and 2e, to form $N_2(A)$. Because of the short lifetimes, $N_2(C)$ and $N_2(B)$ molecules had already decayed before they could reach the reaction cell. Only weak emission from the forbidden Vegard-Kaplan band (radiational decay of $N_2(A)$) was detected in the reaction cell (32). The absence of first and second positive emission indicated that essentially $N_2(A)$ was the dominant species in the afterglow, and generally free from metastable argon atoms or detectable concentrations of $N_2(C)$ and $N_2(B)$ molecules (32).

According to Robertson's work (38) on the reaction of argon afterglow with 14 different gases including N_2, there was no evidence for the presence of ionic Ar species in the afterglow. The observed states of excitation as well as the conditions of the discharge indicated that the excited species were the argon metastables $^3P_2$ and $^3P_0$, with energies 11.72 eV and 11.54 eV, respectively. Thus, no

ionized N_2 molecules are expected to form from the energy transfer by Ar metastable atoms, which carry energy lower than the ionization potential of N_2 (38). With this source of $N_2(A)$, it was possible to examine the reactions between $N_2(A)$ and the analytes of interest.

The concept of Setser's method was followed, while some modifications were made for this experiment. The reaction cell, shown in Figure 5, will be described first. The electric discharge was produced between two hollow copper electrodes in a pyrex tube 7 mm in OD. The surviving Ar metastables passed a light trap located 2 cm downstream of the cathode and intersected with nitrogen gas in the mixing zone, where energy transfer took place to generate $N_2(C)$. In the mixing zone, the first sample port was positioned and an observation quartz window was constructed to monitor reactions. Metastable nitrogen $N_2(A)$ traveled further downstream past another light trap to reach a second sample port. The rationale for two observation zones will be described in the next section. The glass tubes which led the flow from the discharge region to the vacuum pump were all 2.5 cm in OD and painted black on the outside to reduce interference from room light and scattering from the discharge.

A schematic diagram of the pumping system and the gas purification system is shown in Figure 6. The system was evacuated by a Stokes Microvac pump (Model 900-149-11) with a capacity of 2265 L min^{-1}. Cooling water was needed when the pump was in operation. The pump was mounted on a wooden board which was supported on the floor by four plastic shock absorbers to reduce vibration. A built-in 3" diameter flexible metal tube with a 6"

Figure 5
Schematic diagram of the reaction cell for the mechanism study.

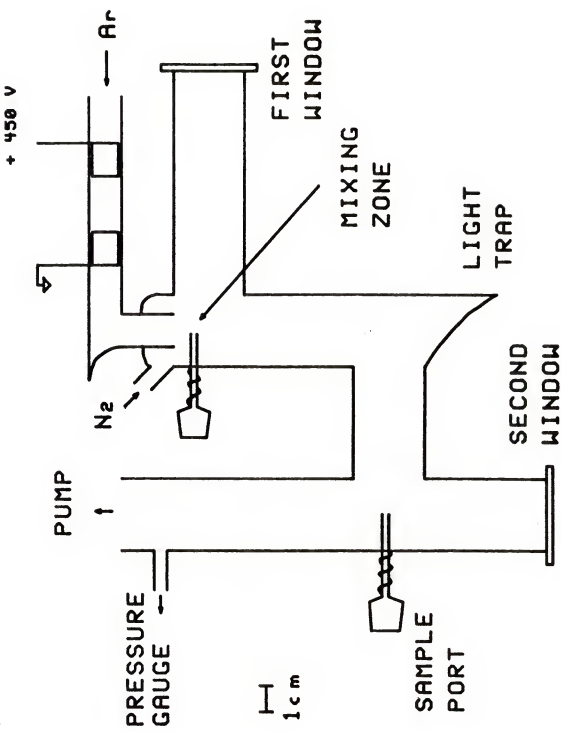
+ 450 V
Ar
FIRST WINDOW
MIXING ZONE
LIGHT TRAP
SECOND WINDOW
N2
PUMP
PRESSURE GAUGE
1 cm
SAMPLE PORT

Figure 6
Schematic diagram of the gas purification system
and pumping system.

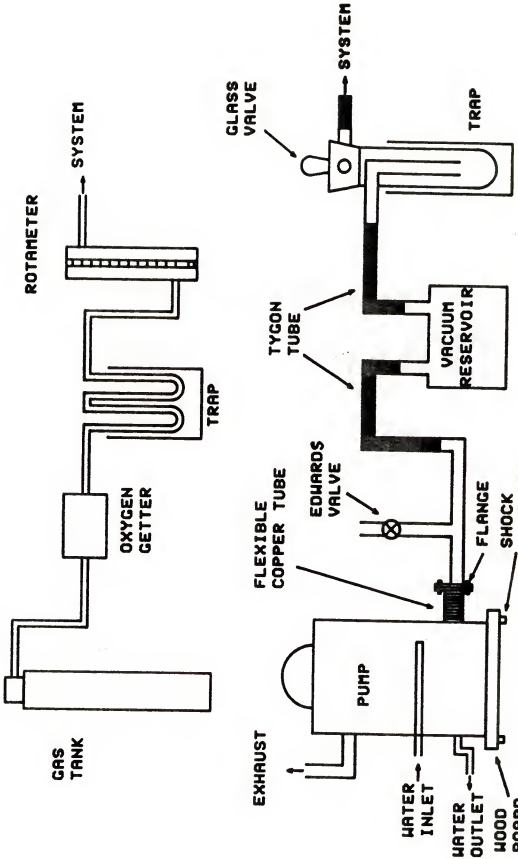
GAS TANK
ROTAMETER
SYSTEM
OXYGEN GETTER
TRAP
GLASS VALVE
SYSTEM
TRAP
TYGON TUBE
VACUUM RESERVOIR
FLEXIBLE COPPER TUBE
EDWARDS VALVE
FLANGE
SHOCK ABSORBER
PUMP
EXHAUST
WATER INLET
WATER OUTLET
WOOD BOARD

diameter flange was mounted on the pump for connecting to the system. A T-shaped copper tube with 1" diameter was made in the departmental machine shop. One end of the T was soldered to another 6" diameter flange which was attached to the flange of the pump with six pairs of bolts and nuts and an O-ring in between. The second end was terminated with a 1" diameter Edwards valve for releasing the vacuum when it was required. The third end of the T-tube attached the system to the pump. A stainless steel cylinder with 6" diameter and 1' length was positioned between the pump and the valve to reduce pumping fluctuation. A large glass valve with a 2 cm diameter bore controlled the vacuum. A glass trap on the bottom of the valve was cooled by dry ice and acetone mixture to keep pump oil from contamination of sample gases. It was found that the NO signal was greatly reduced when the trap was cooled by liquid N_2. The conductance in a trap can be expressed as the following equation (39):

$$c = 9700.\pi.(a_1-a_2)^2.(a_2+a_1).(1/L).(T/M)^{0.5} \qquad (2g)$$

where c = conductance ($cm^3\ s^{-1}$)

a_1 = inner radius of the inner tube of the trap (cm).

a_2 = inner radius of the outer tube of the trap (cm).

L = total length of the trap (cm).

M = molecular weight of the gas in the system (g).

T = absolute temperature in the trap (^oK).

When the trap was filled with liquid N_2, the conductance was reduced

by a factor of $(77/298)^{0.5} = 0.5$. It was necessary to reduce the gas flow rate to keep the optimal pressure and, consequently, the sample signal was also reduced. The concentration of $N_2(A)$ was critically dependent (40) on the pumping rate. Thick wall Tygon tubes with 1" ID and lined with stainless steel wire were employed to connect all the components described above.

The rotameters were calibrated by a mass flow meter (Hastings, Model ALK-50K). A 1.0 V signal from the Hastings meter corresponded to a 1.0 L min^{-1} flow rate. The system pressure was constantly monitored by a pressure gauge (Baratron 321A pressure gauge, MKS Instruments, Inc.). Under a total flow rate of ~50 cm^3 s^{-1} for the dual gas system, the pressure was at ~3.5 torr for the pump used in this work. The mass flow velocity in the cell calculated by the ideal gas law was ~22 m s^{-1} in the 2.5 cm diameter reaction glass cell. The $N_2(C)$ and $N_2(B)$ molecules, with lifetimes of 50 ns and 7 μs, respectively (36), should have already decayed during the time required for travel (~5 ms) from the mixing zone to the second sample port, a distance of 10 cm. The electrodes, which were made of copper sheet with a thickness of 0.1 mm, were spot-welded to platinum wires that were sealed into the discharge tube by uranium glass. The discharge was operated at 450 V DC with a hollow cathode lamp power supply (Heath, Model EU-703-62).

Argon and nitrogen gases were purified by passing the gases over oxygen getters (Matheson disposable gas purifier 6406) to remove trace oxygen and then through two glass wool packed traps cooled by liquid nitrogen to remove moisture and organic materials. The liquid

nitrogen traps for Ar were on the low pressure side, not shown in Figure 6, to prevent condensation of liquid Ar. It was found that the liquid nitrogen traps were very important in the system. When the traps were filled with liquid nitrogen, the nitric oxide signal was at least three times higher than that without liquid nitrogen. A phenomenal purple flame-like plasma from the emission of nitrogen second positive bands disappeared at the mixing zone when the traps were empty, and it came back when liquid nitrogen was added. Since $N_2(C)$ was the precusor of $N_2(A)$, the diminution of the second positive emission meant lower population of $N_2(A)$ for succeeding reactions. The sample tube was connected directly to the gas cylinder when nitric oxide was needed. The gas flow was controlled by a needle valve to obtain the highest signal. The flow rate was not measured. However, the intensity of the NO emission became maximum when the pressure of the system was increased by ~0.01 torr. The intensity was reduced by higher flow rate. For the introduction of benzene and mercury, the sample tube was connected to a teflon vacuum stopcock by a 14/20 ground glass joint. A 10 mL round-bottom flask was attached to the stopcock by another 14/20 ground glass joint. The sample flow of mercury and benzene was controlled by the stopcock. Moderate heating (~35 ^{o}C) of the sample flask by a mantle was needed for benzene evaporation. For the introduction of anthracene, the sample tube was connected directly to the flask with a glass joint, and the flask was heated to ~200 ^{o}C by the mantle. In addition, an auxiliary heating tape was required to keep the sample in gas phase in the connecting tube. Swagelok

fittings were used on the high pressure side of the system, while Cajon Ultratorr fittings were used on the low pressure side.

All measurements were made with a 0.35 m Heath scanning spectrometer equipped with a RCA 1P28A photomultiplier tube (PMT). The PMT signal current was converted into voltage through an electrometer (made in the departmental electronic shop) and the electrometer output was plotted on a strip chart recorder. The monochromator was placed in front of the quartz window without an entrance lens.

The reagents were obtained from the following suppliers:

He: Matheson (High purity grade, >99.995%)

Ar: Matheson (Ultra High purity grade, >99.999%)

N_2: Matheson (Ultra High purity grade, >99.999%)

NO: Matheson (C.P. grade, >99.9%)

Benzene: Fisher Scientific Company (Certified A.C.S.)

Anthracene: Aldrich Chemical Company, Inc. (99.9%)

The flowing discharge gases were purified as described before. Other chemicals were used directly as obtained without purification.

Results

At first, only one observation window was constructed to investigate the reactions between $N_2(A)$ and the sample molecules. After negative results for benzene and anthracene were obtained (described below in the Ar + N_2 experiment), another window (the first observation window in Figure 5) was introduced to examine the possible reactions caused by other excited states such as $N_2(C)$ and $N_2(B)$.

Using He or Ar in the concentric glass tubing discharge system, molecular emission of benzene and anthracene was also observed (discussed in the next chapter); this led to evaluation of He and Ar metastables. Pure He and Ar gases were studied with the same apparatus and under similar conditions as the Ar + N_2 system described below.

Ar + N_2 System

The Vegard-Kaplan bands (radiational decay of $N_2(A)$) (31) which were barely seen by Setser, et al. were not detected in this system. This forbidden emission was cited by Setser, et al. as evidence of the presence of $N_2(A)$ (31). The reason for its absence in our studies was probably due to the very low radiational cross section compared with the collisional decay, and the presence of quenchers such as O_2 in the system. However, the existence of $N_2(A)$ can be indirectly determined by the reaction with NO which gave a considerable intensity of the γ band (see Figure 7); the pertinent reaction is expressed as follow:

$$N_2(A) + NO(X) \rightarrow N_2(X) + NO(A) \qquad (2g)$$

The decay of NO(A) produces the γ band radiation. Apparently, $N_2(A)$ tends either to transfer energy to NO or to decay non-radiationally. Therefore, the system was optimized by monitoring the NO γ band at the second observation zone. A total pressure of 3.5 torr for N_2 and Ar was found to be optimal to obtain high intensity of NO signal. To obtain essentially clean $N_2(A)$, a large partial pressure of N_2

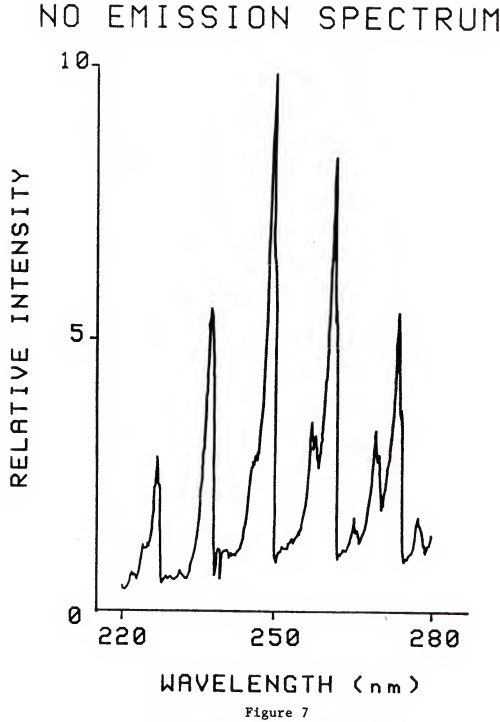

Figure 7
Nitric oxide emission spectrum.

(33-50% of that of Ar) was admitted to the mixing zone to remove any Ar metastables. At the first observation window, the intense N_2 second positive band was detected as expected (see Figure 8).

As mentioned earlier, other N_2 excited state molecules were also objects of interest. Due to the short lifetimes of $N_2(C)$ and $N_2(B)$, they were investigated at the mixing zone where they formed. A flame-like N_2 second positive emission was observed as a cone shape even under full room light. The sample port was constructed at the location where the samples were introduced directly into the emission cone.

Wavelengths of 253.7 nm for Hg, 247.1 nm for NO, 274.1 nm for benzene and 399 nm for anthracene were monitored in Ar + N_2 and other gas systems. Mercury, nitric oxide, benzene and anthracene were examined at both observation windows. The former two species always gave detectable emission while the latter two species did not, as shown in Table I.

The excitation which led to the NO γ band and Hg emission at the second window involved collisions mainly with $N_2(A)$ molecules. This provided the opportunity to examine the excitation mechanism with regard to $N_2(A)$ molecules, and that was unlikely to be achieved by the previous system with the concentric tubes, in which appreciable amount of $N_2(C)$ molecules were present. At the first observation site, a mixture of $N_2(C)$ and $N_2(B)$ existed with evidence of the second positive and first positive emission. The contribution to excitation from these states can not be evaluated separately. However, negative results were always obtained at both windows for

Figure 8
Nitrogen second positive emission spectrum.

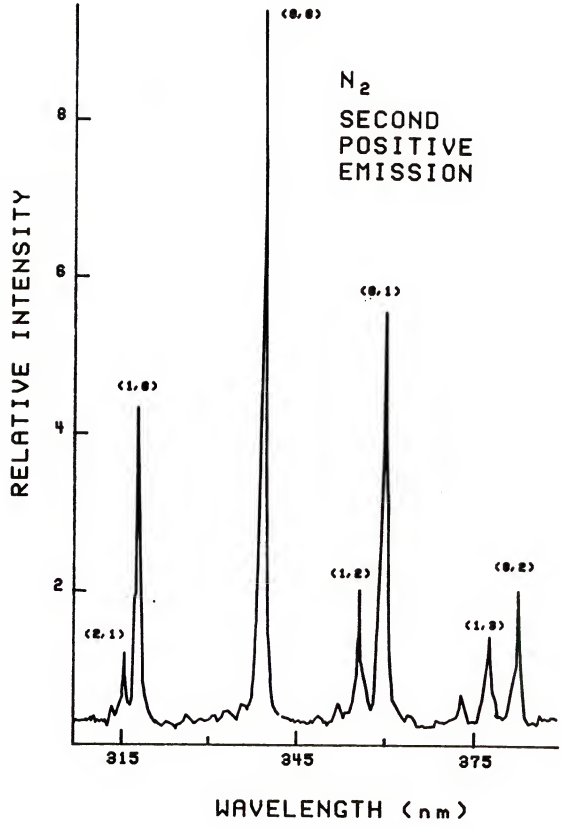
(0,0)
N2
SECOND
POSITIVE
EMISSION
8
6
4
2
RELATIVE INTENSITY
(0,1)
(1,0)
(1,2)
(0,2)
(2,1)
(1,3)
315
345
375
WAVELENGTH (nm)

Table I
Responses of Nitric Oxide, Mercury, Benzene and Anthracene to $Ar+N_2$, N_2, Ar and He Systems

	$Ar+N_2$		N_2		Ar		He
	1[a]	2[a]	1	2	1	2	1
Nitric Oxide	++	++	+++	+++	+	+	-
Mercury	++	++	+++	+++	+	+	-
Benzene	-[b]	-	-	-	-	-	-
Anthracene	-	-	-	-	-	-	-

a) Observation windows, first and second
b) +: Positive response, more + higher intensity
-: No response

benzene and anthracene. Obviously, $N_2(A)$ molecules, as well as $N_2(C)$ and $N_2(B)$, were unable to pump these large organic molecules to their excited singlet states.

N_2 System

Setser and co-workers (31) used the Ar + N_2 system to generate $N_2(A)$ because Ar metastable states ($^3P_0$, 11.54 eV and $^3P_2$, 11.72 eV) carried sufficient energies to excite $N_2(C)$ but not enough to excite higher N_2 metastable states, such as $N_2(E^3\Sigma_g^+)$ (see energy diagram in Figure 4). In the study described above, pure $N_2(A)$ has been shown not to be involved in the excitation of benzene and anthracene. In order to obtain higher concentrations of $N_2(A)$, N_2 gas was excited directly in the discharge instead of by energy transfer from Ar metastables, in which lower efficiency was expected. Under this condition, $N_2(A)$ moved to the reaction cell probably with other metastables of higher excited state. Very weak second positive bands of N_2 were detected at the second window. The formation of $N_2(C)$ molecules was the result of the energy pooling reaction (32):

$$N_2(A) + N_2(A) \rightarrow N_2(C) + N_2(X) \qquad (2h)$$

In the Ar+N_2 system, the second positive radiation was never detected, probably due to the low concentration of $N_2(A)$. With the introduction of NO, the NO γ band was about two orders higher than that observed in the Ar + N_2 system. This implies that the population of $N_2(A)$ could be 100 times higher than that in the Ar + N_2 system. Higher Hg emission signals were further indicative

of the higher concentration of $N_2(A)$ in the system. It was not surprising to see higher signals for NO and Hg at both windows. Even though higher concentrations of $N_2(A)$ existed in this system, negative results for benzene and anthracene were still obtained.

Ar System

While Ar metastables were employed to transfer energy to N_2 (38), it was logical to investigate the reaction between Ar metastables and other molecules, especially after it was shown that fluorescence signals of PAHs could also be obtained in an Ar discharge.

Argon gas was introduced into the discharge tube without the addition of N_2. It was noted that a weak second positive band of N_2 appeared in the background radiation at the first window. The impurity of N_2 could have come from either the Ar gas cyclinder or leaks of the system, and so it was impossible to separate Ar metastables from those of N_2. At the first window, NO and Hg emissions were detected, while there was no emission from benzene and anthracene. At the second window, the same results were obtained. In Robertson's study (38) on the reaction of Ar metastables, no emission of nitric oxide was detected in the presence of the Ar afterglow. Our positive result could arise from the presence of N_2 which was excited and then transferred energy to NO and Hg. At any rate, benzene and anthracene did not emit in the afterglow of Ar.

He Systems

Helium gas was introduced into the discharge tube without mixing with other gases. No emission was observed for any of the four

species at the first window. Collins and Robertson observed very weak γ and β bands radiation when nitric oxide was directed into the He afterglow of a microwave discharge (41). The reason for the negative result for nitric oxide of this work was not clear. However, it could be a result of the low power electric discharge not generating sufficient He metastables for the excitation of nitric oxide.

Discussion

As mentioned previously, the major goal of this study was to examine the role of $N_2(A)$ in the excitation of benzene and its derivatives. From the results for the above four systems, it was concluded that $N_2(A)$ in the discharge afterglow was responsible for the emission of Hg and NO. However, the luminescences of anthracene and benzene were not observed in the afterglow under any condition. Additional studies also showed negative effect of Ar and He metastables for the excitation of benzene and anthracene.

If the cross sections of the reactions between $N_2(A)$ and benzene and anthracene were much smaller than those of the reactions between $N_2(A)$ and NO and Hg, the former two compounds would not be detectable, particularly if the concentration of $N_2(A)$ was low. With N_2 directly in the discharge tube, a higher concentration of $N_2(A)$ was obtained in the afterglow (described in N_2 system); still, no emission from benzene and anthracene was detected. More efforts are needed to get a better system to produce higher concentration of $N_2(A)$. In addition to the above study, a nitrogen laser power supply (AVCO Model C950) has also been employed in order to generate higher

concentration of $N_2(A)$. The experiment will not be presented here in detail because the afterglow was not even able to excite NO molecules, let alone large molecules. According to the comprehensive review on the metastable nitrogen production and energy by Caledonia et al. (42), it is very difficult to efficiently create $N_2(A)$ molecules in discharges at concentration exceeding 10^{13} cm^{-3} because of losses due to the quenching by N atoms and to the $N_2(A)$ pooling reaction.

In the discharge with the concentric glass tubes, there are three dielectric layers, i.e., two pieces of glass and one gas-filled space. When the applied voltage is high enough, these three layers all conduct. However, electric current always travels the path with the least resistance. When a discharge is initiated by the high voltage applied to the inner glass tube, the current looks for return grounds such as the grounded outer glass tube, the vacuum gauge and metal fittings which were grounded through the metal clamps. In fact, discharge sparks are observed at these spots. In addition, the "afterglow" is deflected by a magnetic bar (also reported by Allen, et al. (43)). The so-called afterglow in the reaction cell, therefore, is considered as an extended discharge.

The studies performed in this chapter were designed to investigate the reaction of samples with a clean $N_2(A)$ source. The final experimental arrangement was different from the set-up with the concentric glass tubes. Therefore, the previous apparatus was modified with a tungsten wire sealed in the light trap close to the discharge tube and grounded, as shown in Figure 9. The second

positive bands were not detected in the reaction cell during the discharge. Apparently, the discharge was intercepted by grounded tungsten wire and thus, unable to extend into the reaction cell. Nitric oxide was introduced into the reaction cell, and no emission was observed. The uncharged $N_2(A)$ molecules should not be stopped by the grounded wire in the light trap. With a flow rate of 5 mL min^{-1} (as will be described in chapter III), diffusion became more rapid than the linear velocity of the gas in the cell (26). Calculated by the ideal gas law, the travel time for gas molecules from the discharge tube to the sample introduction port was ~0.2 s with 1.25 cm diameter light traps and ~10 cm distance from the discharge tube to the sample cell. $N_2(A)$ molecules were lost either to spontaneous de-excitation or to de-excitation by gas phase collisions and collisions with the glass wall (41). The concentration of the surviving $N_2(A)$ was lower than the detectable concentration by reaction with NO molecules.

Although the emission of the second positive bands was dominant in the reaction cell with the concentric discharge tube, $N_2(C)$, $N_2(B)$ and $N_2(A)$ molecules were by no means the only species existing in the extended discharge. The average electron energy estimated by Allen, et al. (26) was about 11.4 eV at 1 torr. A broad distribution of electron kinetic energy would mean that some would exceed the ionization potential (15.45 eV) of N_2. Even though no emission of N_2^+ was observed, the ground state N_2^+ could still be present. The emission system of N_2 is so complex (33), that there is no easy method to evaluate the contribution from the individual species, such

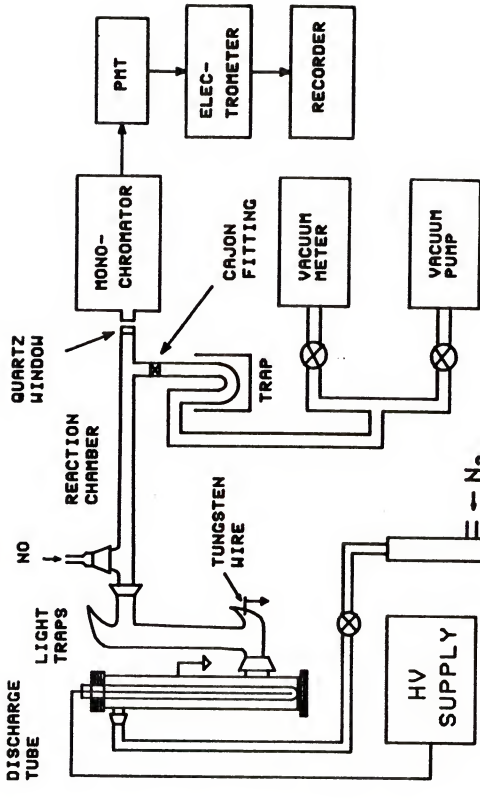

Figure 9

Block diagram for the excitation mechanism study modified with an extra grounded tungsten wire in the light trap.

as ionic molecules, nitrogen atoms, excited molecules and metastable molecules, in the excitation process. However, under controlled conditions in the Ar + N_2 system, no emission of benzene and anthracene was observed was observed in the presence of $N_2(A)$, $N_2(B)$ and $N_2(C)$ molecules.

CHAPTER III
MOLECULAR SPECTRAL ANALYSIS

Methods of Analysis

Temperature Determination

Temperature is one of the important diagnostic parameters to characterize a plasma. Excitation temperature (44,45) can be measured by applying Boltzmann's law, either by using the spectral lines of the fill gas or the spectral lines from the elements introduced into the plasma. An external heating device is needed for the sample vaporization and atomization if involatile metal salts are to be introduced into the electric discharge plasma; otherwise, volatile metal compounds such as metal hydrides can be introduced directly. In this work, Ar and He spectral lines were used, because there are well documented spectral parameters in the literature for these gases.

The intensity of a spectral emission can be expressed as the following equation (46):

$$I = (h.\nu.N.g.A/Q) \cdot \exp(-E/kT) \qquad (3a)$$

where I = intensity of the line.

h = Plank's constant.

ν = the frequency of the line.

N = the number of free atoms.

g = statistical weight of the level.

A = transition probability for the line.

Q = partition function of the atom.

E = excitation energy.

k = Boltzmann constant.

T = absolute temperature.

The slope P of the straight line obtained by plotting the graph of log $I\lambda/gA$ as a function of E gives the value to calculate the temperature T by the equation $P = 0.625/T$.

The choice of the spectral lines is made, first, within a limited range of wavelengths in order to reduce the influence of the non-uniformity of the spectral response of the dispersive system and of the photomultiplier (47). Secondly, the agreement of the transition probability values from literature has to be taken into consideration (47). Eight lines (3P-1S transitions) of Ar were chosen from different sources (48-53), as listed in Table II. Five lines (402.62, 447.15, 471.32, 492.19 and 501.57 nm) were chosen for He; the transition probabilities were obtained from the NBS Reference Data (54). The straight lines of the plots were determined by the least squares method. The experiments were performed at different applied voltages to determine the effect of discharge voltage on the excitation temperatures.

Table II
Transition Probabilities of Ar

Wavelength (nm)	E[a] (cm^{-1})	g[b]	Transition probabilities ($10^7 s^{-1}$)[c]					
			I	II	III	IV	V	VI
425.118	116660	3	0.0079	0.0089	0.0132	0.0095	0.0076	0.0075
425.936	118871	1	0.36	0.3665	0.45	0.409	0.32	0.3643
426.629	117183	5	0.028	0.0265	0.036	0.0328	0.023	0.0294
427.217	117151	3	0.071	0.0688	0.090	0.087	0.063	0.0769
430.010	116999	5	0.034	0.0318	0.042	0.0382	0.031	0.0366
433.356	118469	5	0.049	0.0506	0.074	0.060	0.048	0.0551
433.534	118460	3	0.040	0.0308	0.044	0.046	0.029	0.0385
434.517	118407	3	0.028	0.0273	0.041	0.0334	0.022	0.0278

a : Excitaion energy.
b : Statistical weight.
c : Transition probabilities from six authors,
    I. Gericke (48)
    II. Malone (49)
    III. Corliss (50)
    IV. Wiese (51)
    V. Wende (52)
    VI. Wujec (53)

Spectral Measurement of Polycyclic Aromatic Hydrocarbons

Molecular spectra

The analysis of PAHs has become a very important research area because of their carcinogenic properties (55-57). These compounds are released from volcanoes (58,59), forest fires (60) and incomplete burning of organic material (61,62). The techniques for the determination of these compounds include mass spectrometry, gas chromatography, high performance liquid chromatography and other modern analytical methods (63). In this laboratory, a number of luminescence techniques have been applied for the analysis of PAHs, including room temperature phosphorimetry (64), low temperature luminescence and photoacoustic spectrometry (65), and constant energy synchronous luminescence spectrometry (66). Active nitrogen-induced chemiluminescence is another approach (16) which has eventually led to a study of electric discharge induced luminescence and this dissertation.

Because of the limited volatility of most PAHs, samples must be kept in the gaseous phase by elevated temperatures. When using a scanning optical system, the analyte must be introduced into the flowing system at a constant rate to obtain spectra of high fidelity. Alternatively, a non-scanning multichannel detector can be used for a simultaneous wavelength measurement. A photodiode array (PDA) detector was employed in this study with software capabilities for background subtraction and other data reduction calculations.

Quantitative measurements

A reproducible sample introduction device was required for quantitative measurements. Since the analyte was measured in the gaseous phase, a gas chromatograph (GC) was employed for sample introduction. Solutions of PAHs and other hydrocarbons in heptane were prepared. Analyte solutions were injected into a GC with an empty glass column. The eluted analyte was directed into the electric discharge plasma.

Experimental

The Discharge Tube and Reaction Cell

The discharge tube consisted of two concentric pyrex glass tubes. The outer tube was 16 cm long, with 9 mm in outer diameter (OD) and 7.5 mm in inner diameter (ID). The inner tube was 18 cm long, 5 mm in OD and 4 mm in ID. The glass tubes were held in place and isolated by two Macor ceramic spacers. These spacers were sealed by epoxy to make them vacuum tight. Flow gas was introduced to the tube through a 10/30 ground glass joint. High voltage was applied to a copper wire which was placed in the inner tube that was filled with saturated NaCl aqueous solution. The outside of the outer tube was painted with Ni paint, wrapped with conducting tape and grounded.

Since the ground of the outer glass of the discharge tube was unable to draw all the current, the plasma extended over the whole vacuum system wherever metal parts were present (as described in Chapter II). A Cajon fitting which was located between the reaction cell and the dry ice cooled trap was grounded, as shown in Figure 10, and the plasma was therefore confined in the reaction cell. The

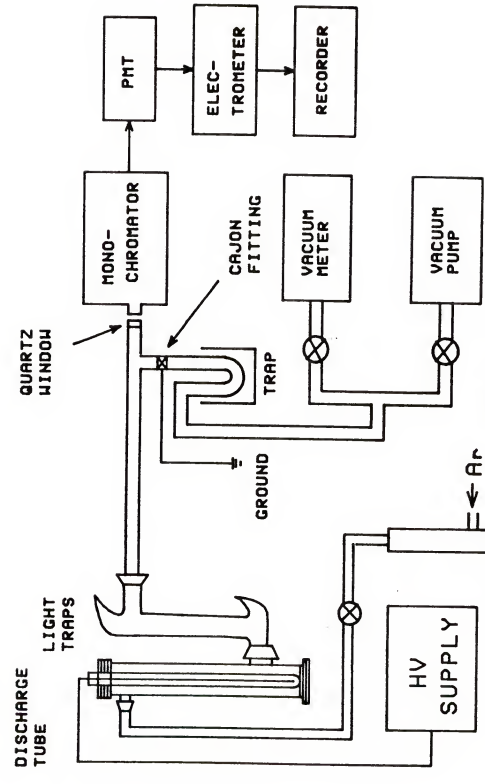

Figure 10
Block diagram of the electric discharge apparatus for temperature determination.

reaction cell was 15 cm long and 25 mm in OD. A quartz window was glued to the open end for the spectral measurement.

The system was evacuated by a pump (3/4 HP VacTorr, GCA/Precision Scientific) at a flow rate of ~5 ml min^{-1} to keep the pressure at ~1 torr. The pressure was monitored by a Baratron 321A pressure guage (MKS Instruments, Inc.).

Argon was introduced to the system for the temperature determination. The experimental diagram is shown in Figure 10.

When molecular spectra of PAHs were to be measured, a heating tape was needed, as shown in Figure 11, to evaporate samples into gaseous phase. Usually the temperature was kept at ~200 ^{o}C, except for samples with high vapor pressure such as naphthalene which sublimed in the vacuum without heating. Samples of about 1 mg were introduced directly into the reaction cell at atmospheric pressure through the sample port. The system was then pumped down to the desired pressure.

Several changes were made for quantitative measurements, as shown in Figure 12. An empty glass tube in a Shimadzu model 6A GC was connected by a 5/20 ground glass joint to the discharge zone. The connecting tube from the GC outlet to the discharge was wrapped with heating tape. The sample stream was directed by a 7 mm OD tube and intercepted vertically by the discharge plasma. A shorter residence time for sample in the discharge was expected in this configuration.

The glassware for sample solution preparation was soaked overnight in cleaning solution (Micro Laboratory Cleaning Solution),

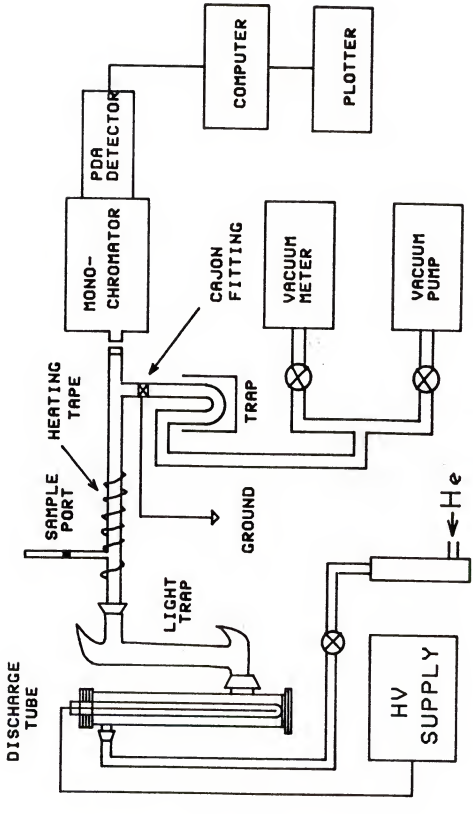

Figure 11
Block diagram of the electric discharge apparatus for molecular spectral measurements.

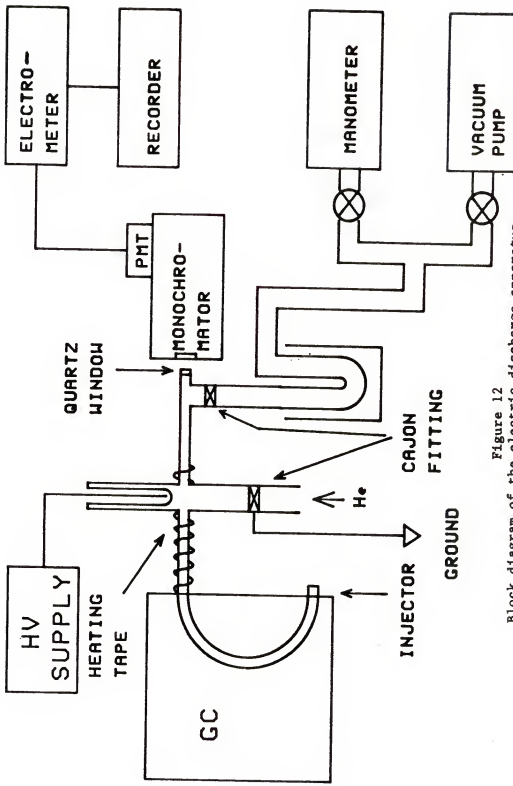

Figure 12
Block diagram of the electric discharge apparatus for quantitative measurements.

then rinsed with de-ionized water, and finally with Barnstead de-ionized water. Twenty-five- to fifty-part-per-million (ppm) stock solutions of the PAHs and hydrocarbons in heptane were prepared. Solutions of lower concentrations were prepared by serial dilution of the stock solution.

High Voltage Power Supply

The home-made AC power supply consisted of a 15 kV neon sign transformer. The circuit is shown in Figure 13. One terminal of the high voltage secondary was used for the output; the other one was disconnected and protected from shorting by a teflon cap. The discharge voltage was read out through a 1000:1 voltage divider and the current was monitored across a 101 Ω precision resistor which was in series with the ground return. The primary coil of the neon sign transformer was powered by a Variac with voltage ranging from 0-110 V AC to give the secondary coil voltages 0-7.6 kV AC. A line filter was inserted across the power line to minimize pickup of noise generated by the discharge. All electric components were built on a bread board which was housed in a 13.5" by 5.5" by 4" aluminum box which helped to confine the RF noise generated by the transformer. All components were kept at secure distances to avoid any possible breakdown. An opening on the box provided the convenience of measuring the applied voltage and the current of the output. Two pairs of plug terminals built on the bread board were located right at the window. One pair of the terminal was built across the 40 kΩ resistor (see Figure 13) and the other one was across the 101 Ω resistor. The test leads of a multimeter were plugged into the

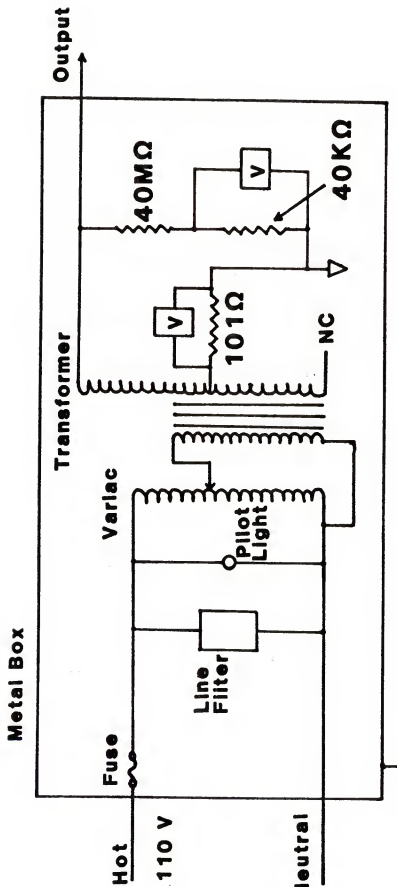

Figure 13
Circuit diagram of high voltage power supply.

terminals for the voltage and current mensurements. The opening was closed after these measurements. The high voltage output line was first protected by a 1/4" diameter polyethylene tube and then shielded by a 1/2" diameter copper tube to suppress RF noise.

Detection Systems

A single channel system was composed of a mechanical scanning spectrometer, photomultiplier tube and read-out device. This system has been described in Chapter II.

A photodiode array (PDA), Tracor Northern model TN-6122, was employed for the multichannel detection. Low light levels were measured by the amplification of an image intensifier. The spectral range was primarily from 350 nm to 850 nm with a maximum sensitivity at about 450 nm. The sensitivity of UV response was improved by a scintillator layer on the detector head. The analog signals from 1024 diodes were electronically scanned and digitized by an analog to digital converter (ADC) for further data manipulation. The ADC resolution could be chosen from 11 bit to 14 bit that provided a maximum dynamic range of 16384:1. The spectral intensity was expressed as counts. It is approximately 5000 photoelectrons per count. Temperatures at the detector colder than room temperature could be obtained by a built-in liquid cooling facility to reduce dark current.

The PDA was controlled by a Tracor Northern TN-6500 Rapid Scan Controller. This spectral controller provides all control signals and support electronics for the detector head. In addition, it includes dual microprocessors for the storage of spectral data,

operational control, data processing and interfacing with all external systems such as display, floppy discs, printer and plotter.

The flat-field monochromator (Instruments SA, Inc., model UFS-200) was designed for PDA detectors. With a 200 grooves mm^{-1} grating, it covered the wavelength range from 200 to 800 nm with a linear dispersion of 24 nm mm^{-1}. Three fixed slit widths were provided; 50, 100 and 250 μm, respectively. An aluminum adaptor was made by the department machine shop to install the TN-6122 PDA on the monochromator. With eight adjustable set screws, the detector can be properly positioned and focused on the spectrometer.

Chemicals

The gas reagents used in the experiment have been described in Chapter II. The sources of PAHs and hydrocarbons are as follows:

Anthracene, 9-Methylanthracene 2,3-Dimethyl-Naphthalene Carbazole, Naphthalene, Pyrene	Eastman Kodak Rochester, NY
Benzo(a)pyrene, Benzo(e)pyrene Benzo(k)fluoranthene, Perylene	Aldrich Chemical Co. Milwaukee, WI
Coronene	Fluka AG, Buchs Switzerland
Fluoranthene	Chem Service Media, PA
Heptane	American Burdick and Jackson Muskegon, MI

Results and Discussions

Excitation Temperatures

The results of the measurement are listed in Table III. Each slope of log $I\lambda/gA$ versus E was calculated by linear least squares

Table III

Excitation temperatures obtained by Ar and He lines.

Current(mA)	0.83	1.40	2.00	2.60
Applied Voltage(V)	2100	3500	5020	6260
Ar(Gericke) (48)[a]	$(3.4\pm1.2)\times10^3$[b]	$(3.5\pm1.3)\times10^3$	$(3.4\pm1.1)\times10^3$	$(3.5\pm1.2)\times10^3$
Ar(Malone) (49)	$(3.96\pm0.35)\times10^3$	$(4.14\pm0.50)\times10^3$	$(4.19\pm0.42)\times10^3$	$(4.29\pm0.66)\times10^3$
Ar(Corliss) (50)	$(3.7\pm0.7)\times10^3$	$(3.8\pm0.6)\times10^3$	$(3.7\pm0.5)\times10^3$	$(3.8\pm0.6)\times10^3$
Ar(Wiese) (51)	$(3.3\pm0.9)\times10^3$	$(3.4\pm0.9)\times10^3$	$(3.5\pm0.9)\times10^3$	$(3.5\pm0.9)\times10^3$
Ar(Wende) (52)	$(4.0\pm0.8)\times10^3$	$(4.2\pm1.2)\times10^3$	$(4.0\pm1.0)\times10^3$	$(4.2\pm1.3)\times10^3$
Ar(Wujec) (53)	$(3.33\pm1.17)\times10^3$	$(3.43\pm1.36)\times10^3$	$(3.53\pm1.23)\times10^3$	$(3.54\pm1.38)\times10^3$
He(NBS) (54)	$(3.74\pm1.29)\times10^3$	$(3.57\pm1.17)\times10^3$	$(3.69\pm1.22)\times10^3$	$(3.72\pm1.26)\times10^3$
Average	$(3.63\pm0.29)\times10^3$[c]	$(3.72\pm0.33)\times10^3$	$(3.70\pm0.26)\times10^3$	$(3.79\pm0.33)\times10^3$

a : Reference of the source of the transition probability.
b : Confidence interval at 95%.
c : The average temperature with standard deviation of seven measurements.

method with a single data set. The confidence intervals b of the slope at 95% were also obtained. The temperature was then computed with the equation: $T = 0.625/(P \pm b)$.

The major difficulty in measuring temperatures in a flame or plasma is the reliability of the available transition probabilities. These values for many elements are poorly known. One author has estimated that these values are known to within 25% (67), while it is very common to find more than 40% deviation (48-53). The excitation temperatures calculated vary with the transition probabilities of the Ar lines from different sources (Table II). However, these values are of the same magnitude within the measurement uncertainty. Temperatures measured by He lines show the same magnitude as by Ar lines within the uncertainty. In each set of data, the temperature is very insensitive to change of the applied voltage and the resultant discharge current. This was also true in a glow discharge reported by Mehs and Niemczyk (68). With increasing current, increasing intensities of individual line was observed. Higher currents created more excited atoms, but did not significantly change the population ratio between those excited states.

Discharge Characteristics

In an electric circuit, electrons always follow the shortest routes (lowest resistance). As mentioned before, the plasma generated by the glass electrode discharge was attracted by metal parts in the system, downstream as well as upstream of the gas flow. The ground at the outer glass tube did not draw all the current. To investigate the influence of the grounding on the discharge, currents

were measured when either the glass wall or the Cajon fitting was grounded. The results, shown in Figure 14, were obtained at 1.03 torr under N_2 gas. The current of the discharge increased almost linearly from 4.5 to 7.0 kV at a slower rate, then more rapidly above 7.0 kV. The impedance of the system was reduced with the metal Cajon fitting grounding rather than grounding through glass; therefore, a higher current was expected.

In addition to the applied voltage, pressure plays an important role in the system. At fixed applied voltage (7.5 kV), the discharge current was measured at different pressures. The intensity of the second positive emission of N_2 at the peak wavelength at 337.1 nm was measured as a function of the pressure. The current as well as the emission intensity increased as the pressure went up from low pressure and reached a peak approximately in the neighborhood of 1 torr, as shown in Figure 15, then decreased as the pressure further increased. Although the intensity of the emission dropped off more rapidly than the current at increasing pressure, both of these parameters peaked at approximately the same pressure. This type of intensity curve was not made for individual PAHs; however, most measurements were made at 1 torr with applied voltage at 7.5 kV.

Spectral Measurements

Wavelength calibration

A mercury pencil lamp was employed to calibrate the wavelength of the PDA detector (a 100 μm entrance slit was used). A neutral density filter was placed in front of the spectrometer to reduce the light intensity in order to protect the detector when the intensifier

Figure 14

Discharge current as a function of applied voltage when Cajon fitting or the outer concentric glass tube was grounded.

Figure 15
Discharge current and nitrogen emission at 337.1 nm
as a function of the system pressure at applied voltage 7.5 kV.

RELATIVE INTENSITY
0
20
40
60
80
100
0
2
4
6
8
10
12
PRESSURE (TORR)
0.28
0.56
0.84
1.12
1.40
CURRENT (mA)
CURRENT
INTENSITY

was turned on. The mercury emission line at 253.7 nm as well as Ar emission lines were well documented (69). The detector head was rotated back and forth slightly at the connection with the spectrometer until the sharpest and narrowest emission lines were obtained; then the set screws were all tightened. Following the standard procedures to input the wavelength of the individual line with the corresponding diode, the diode numbers were converted into nm, cm^{-1}, and several other spectral energy expressions. The data file of the calibration spectrum was stored on floppy disc to be recalled whenever needed. A new calibration was required only when a change of the optical system was made.

Dark current

Although dark current of the detector may be corrected for by background subtraction, it is still necessary to minimize it. The output current (signal) of the detector can be saturated if it reaches the maximum value of the elecron-hole pairs that the diodes can create. The exposure time to the light source may have to be reduced to avoid saturation because of the high dark current which also contributes to the signal. Therefore, the electronic system may lose the capability to detect low light levels due to the short exposure time which is limited by the high dark current.

There is a thermoelectric cooling device in TN-6122 detector to cool it below room temperature. A thermostat can be set by an adjustment on the detector, and the temperature is monitored by a thermocouple. Lower temperatures can be obtained with coolant to remove heat rather than with air cooling.

Tap water was used in this work as the cooling agent. The averages of the relative dark current for all 1024 diodes were 36, 13, 3.9, 1.2 and 1 at temperatures of 22.5, 9.8, -2.4, -17.5 and -18.7 ^{o}C, respectively, giving a significant reduction of the dark current. All the measurements were made at the lowest temperature possible.

Background radiation

Nitrogen and helium were considered for use as the fill gas because one of these two gases was to be chosen as the GC carrier gas for quantitative analysis. Second positive bands of N_2 were already known as very intense emission between 300 and 400 nm. Background emission from He was then also examined. Figure 16 shows the emission of N_2 and He from 250 to 550 nm, the wavelength range of interest for the luminescence of most PAHs. These two spectra were obtained under the same experimental conditions at a pressure of 1 torr. The system was flushed with the gas of interest for at least 15 min before taking any measurement. Between 250 and 400 nm, the nitrogen second positive bands were the dominant emission under N_2 gas, while there were three major bands at 395, 450 and 505 nm for He with much lower intensity compared with the nitrogen second positive bands. Therefore, helium was chosen to be the flow gas. The stability of the discharge was examined by monitoring the emission of He. Spectra were measured under the same conditions every 10 s for about 10 min. Fluctuation of the peak intensity was about 5%; occasionally, a 10% variation occurred.

Figure 16
Background radiation of nitrogen and helium
at wavelengths between 250 and 550 nm.

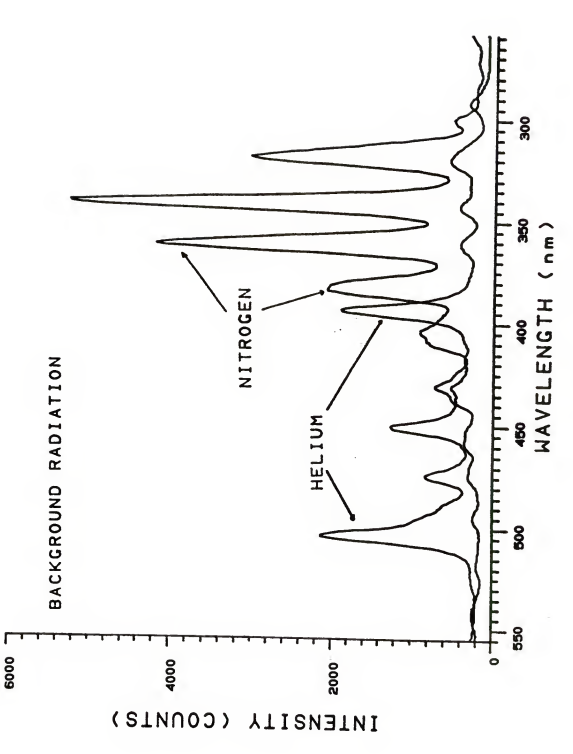
INTENSITY (COUNTS)
6000
4000
2000
0
BACKGROUND RADIATION
NITROGEN
HELIUM
550
500
450
400
350
300
WAVELENGTH (nm)

Molecular spectra and background compensation method

The measurement of the spectrum of anthracene will be described in detail as an example for other compounds. Helium emission without sample (blank) was first recorded at an exposure time of 3 s. The TN-6500 controller was set at the sequential measurement mode. Sample introduction was described previously in the experimental section. When the heating tape was turned on, measurement was also started. As the temperature of the reaction cell was increasing, the sample evaporated into the discharge and was excited. The spectra were measured at the same exposure time as the blank, with 1 s delay between each measurement. The intensity of anthrancene emission increased at first as more sample vaporized into the reaction cell and then gradually decreased as analyte molecules were pumped out of the cell. Since it took 3 s for exposure to the emission source and 1 s delay between each measurement, 4 s elapsed for each spectrum. The spectra of the sequential measurement were shown in Figure 17. Spectrum No. 13 with the highest intensity at 370 nm was chosen for background subtraction. Spectra of the blank and the anthracene are drawn in Figure 18 on the same coordinates to show the difference. As can be seen in Figure 18, the intensity of the He lines in the blank at 588.4, 673.1 and 717.5 nm was more than 10% higher than that of the sample, and more than 7% higher at 501.1 and 743.3 nm. This intensity variation at the He emission was first considered as the fluctuation of the plasma. However, after measuring all samples, it was found that the intensity of the blank at He emission wavelengths was always higher than that with sample. The variation was

Figure 17
Sequential measurement for anthracene with an exposure time of 3 s and 1 s delay between each measurement.

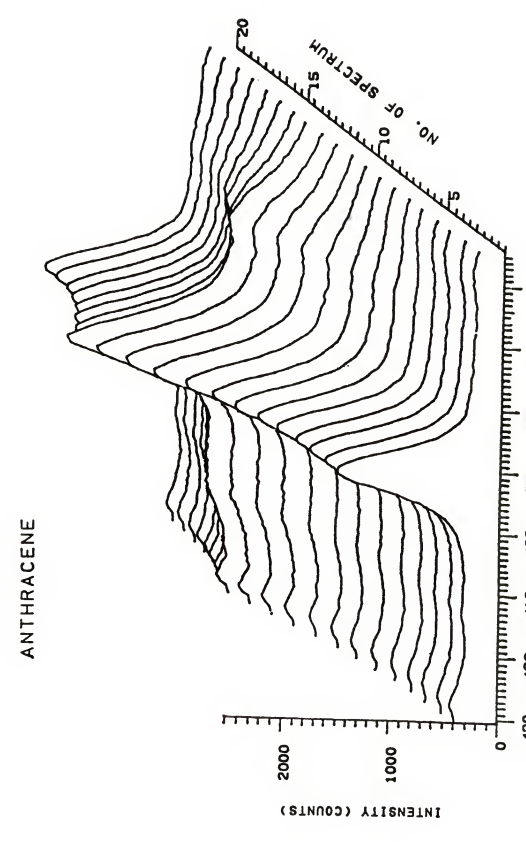
ANTHRACENE
INTENSITY (COUNTS)
2000
1000
0
430
420
410
400
390
380
370
360
WAVELENGTH (nm)
NO. OF SPECTRUM
20
15
10
5

Figure 18
Comparison between the spectrum of the blank and the spectrum with the presence of anthracene.

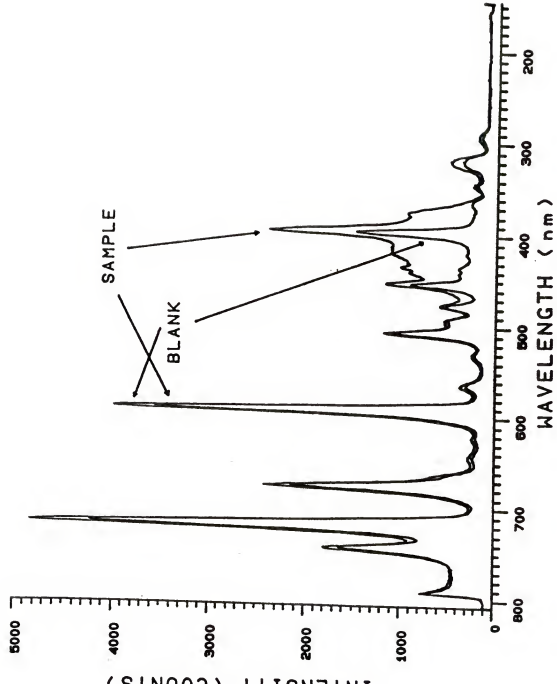
INTENSITY (COUNTS)
5000
4000
3000
2000
1000
0
800
700
600
500
400
300
200
WAVELENGTH (nm)
SAMPLE
BLANK

apparently systematic rather than random. The lowering of the intensity at He emission wavelengths was then considered as a result of the introduction of analyte. In other words, the presence of analyte was a disturbance to the He plasma. An adjustment was made to compensate the background variation caused by the disturbance of the analyte to the discharge. Under the assumption that the relative helium emission peak intensities remained constant under all the conditions, a compensation for analyte quenching of He emission was made by taking the ratios of each He line in the presence and absence of analyte to equalize the intensities of the peak at each wavelength. The ratios of the peak intensity in the absence and presence of analyte were 1:0.9162, 1:0.8889, 1:0.8876, 1:0.8731, and 1:0.9241 at the above five He emission wavelengths, respectively. Each datum in the spectrum of the blank was multiplied by the average ratio 0.8980 and subtracted from the spectrum of the analyte. The corrected spectrum of anthracene is shown in Figure 19.

The variation of the intensity of the He background peaks was examined for all twelve compounds. For those He peaks that did not overlap with the analyte emission, the ratios of analyte/blank were measured. The results are listed in Table IV. The reduction of the peak intensity of the He emission can range from 5% to 40% with the presence of analytes. A direct background subtraction without compensation may cause serious error in background correction. Accordingly, the spectra of the rest of the compounds were obtained by the background compensation method, as shown in Figures 20-25.

Figure 19
Spectrum of anthracene after background correction.

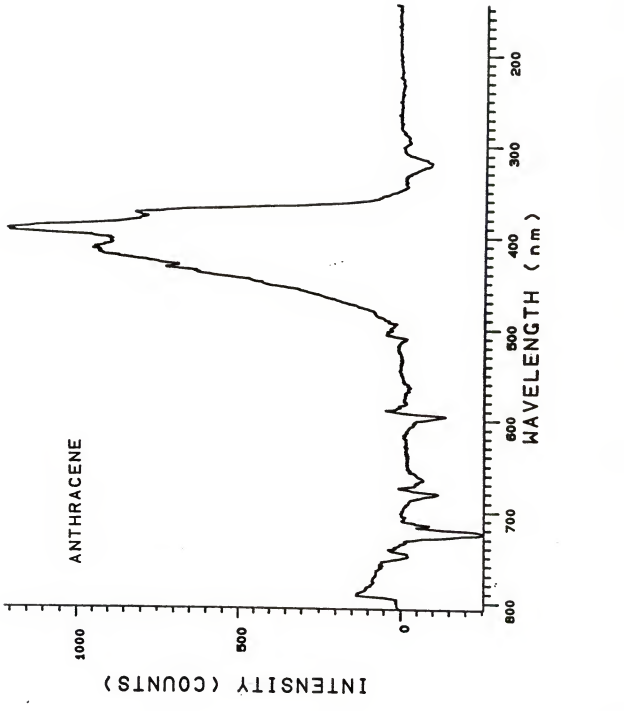
ANTHRACENE
INTENSITY (COUNTS)
1000
500
0
800
700
600
500
400
300
200
WAVELENGTH (nm)

Table IV
The ratio of He emission with analyte present to He emission with blank for 5 different He wavelengths

Analyte	Wavelength (nm)					Mean	Standard deviation
	745.3	720.8	675.8	589.1	502.4		
Anthracene	0.9241	0.8731	0.8876	0.8889	0.9162	0.8980	0.0214
Benzo(a)pyrene	0.8246	0.8038	0.8470	0.8137	*	0.8223	0.0185
Benzo(e)pyrene	0.8549	0.8478	0.8775	0.8639	0.8778	0.8644	0.0134
Benzo(k) fluoranthene	0.9321	0.9212	0.9654	0.9852	*	0.9509	0.0296
Carbazole	0.8642	0.8409	0.8931	0.8488	0.8695	0.8633	0.0202
Coronene	0.8770	0.8630	0.9137	0.8840	*	0.8844	0.0214
2,3-Dimethyl-naphthalene	0.6183	0.6272	0.6390	0.6529	0.6010	0.6277	0.0198
9-Methyl-anthracene	0.7946	0.8092	0.8503	0.8001	*	0.8136	0.0252
Fluoranthene	0.7235	0.7627	0.7156	0.7585	0.7321	0.7385	0.0211
Naphthalene	0.5965	0.6104	0.6083	0.6690	0.5726	0.6114	0.0356
Perylene	0.6238	0.6374	0.6585	0.6156	0.6337	0.6338	0.0162
Pyrene	0.7713	0.7439	0.7731	0.7814	0.7876	0.7715	0.0167

* : Wavelength overlapped with the luminescence of the sample.

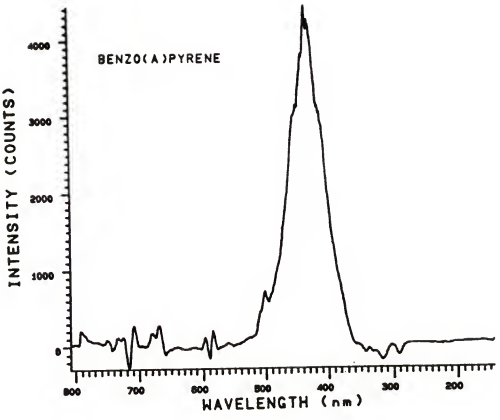

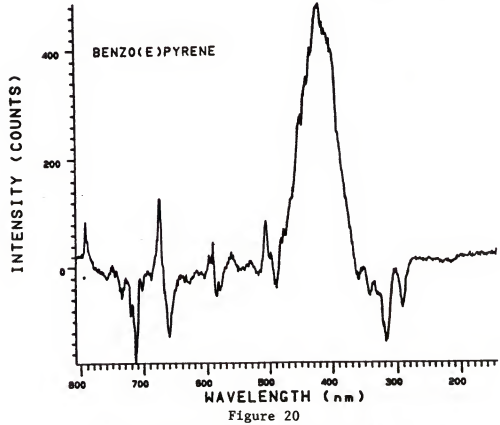

Figure 20
Spectra of benzo(a)pyrene and benzo(e)pyrene.

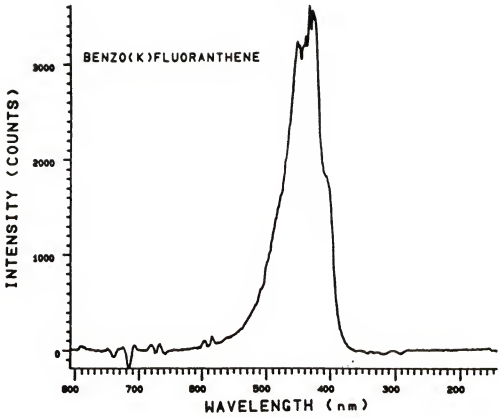

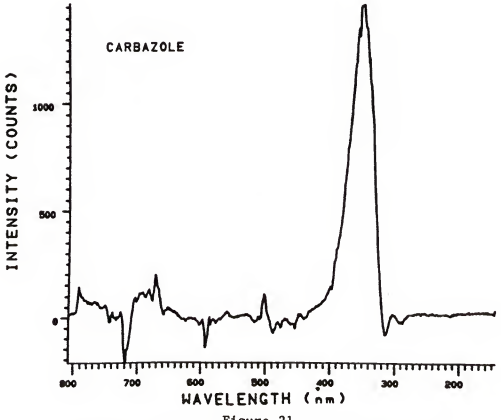

Figure 21
Spectra of benzo(k)fluoranthene and carbazole.

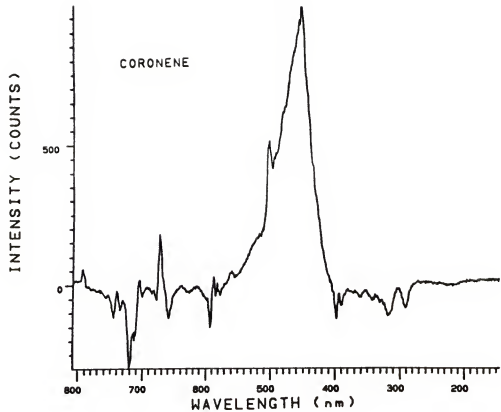

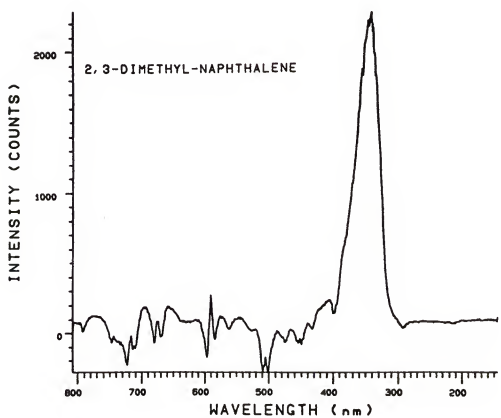

Figure 22
Spectra of coronene and 2,3-dimethyl-naphthalene.

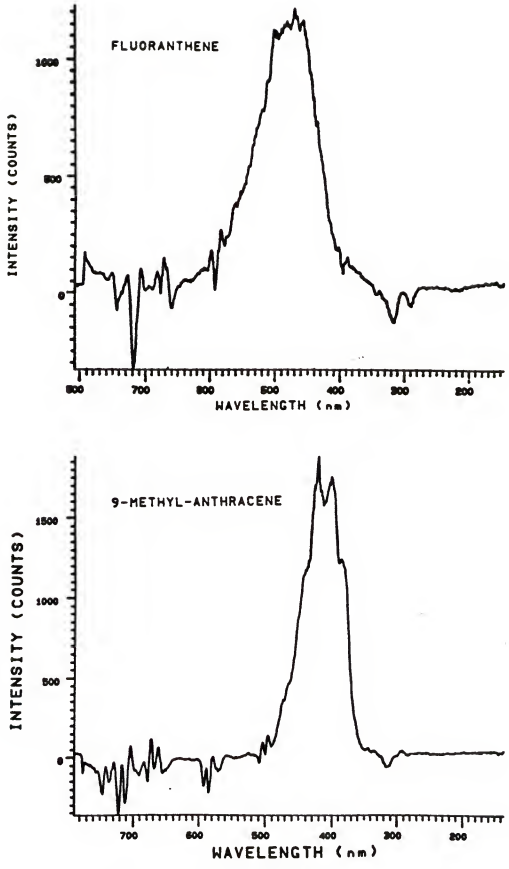

Figure 23
Spectra of fluoranthene and 9-methyl-anthracene.

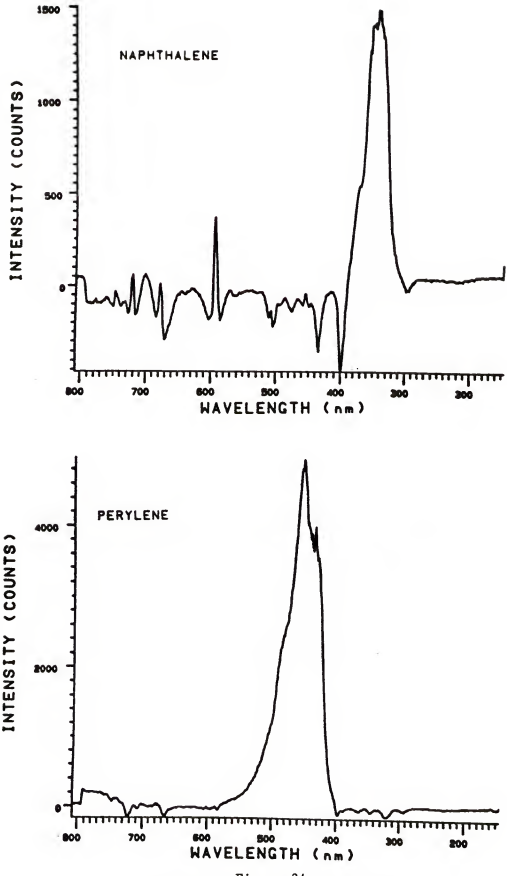

Figure 24
Spectra of naphthalene and perylene.

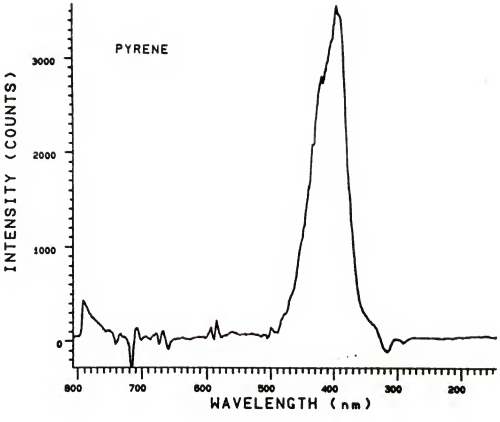

Figure 25
Spectrum of pyrene.

Unfortunately, the relative peak intensities from the emission of He were not constant, as shown in Table IV. The background could be either over-corrected or under-corrected, as shown in each spectrum at the wavelength regions of He emission. However, the presence of the bumps and troughs in the background, for example, the bump at ~590 nm and trough at ~595 nm for anthracene, are not well understood. Apparently, He emission with the presence of analyte was not proportionally lowered at each individual wavelength, and thus both bumps and troughs were present in the region with only one He peak, instead of either one bump or one trough. The presence of bumps and troughs could also result from wavelength shifts or band broadenings. For example, for anthracene the background emission of the blank was multiplied by 0.898 (the average He peak intensity ratio of analyte/blank) to mimic the condition with the presence of anthracene. Both spectra of the analyte and the compensated blank are shown in Figure 26. Helium emission of analyte and blank match very well from 500 to 750 nm. The emission of the blank was under-corrected above 750 nm and below 350 nm. This phenomenon was also observed for other analytes, see Figure 20-25. The variation of the He emission could not be examined in the region from 350 to 500 nm where analyte emitted and overlapped with the He emission.

The wavelength coordinate is expanded, as shown in Figure 27, in order to look more closely at the He peak at ~590 nm. A blue shift is observed for the He emission with the analyte. However, this was not the case for other analytes, for example, benzo(a)pyrene given

Figure 26
Comparison of the spectrum of the blank after
background compensation to the spectrum with anthracene.

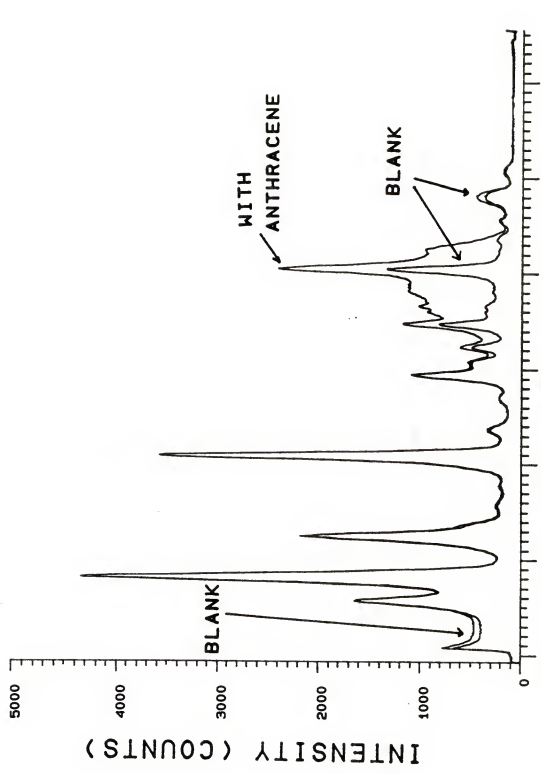
INTENSITY (COUNTS)
5000
4000
3000
2000
1000
0
BLANK
WITH ANTHRACENE
BLANK
800
700
600
500
400
300
200
WAVELENGTH (nm)

Figure 27
Helium emission at 585 nm with the presence
of anthracene and the compensated blank.

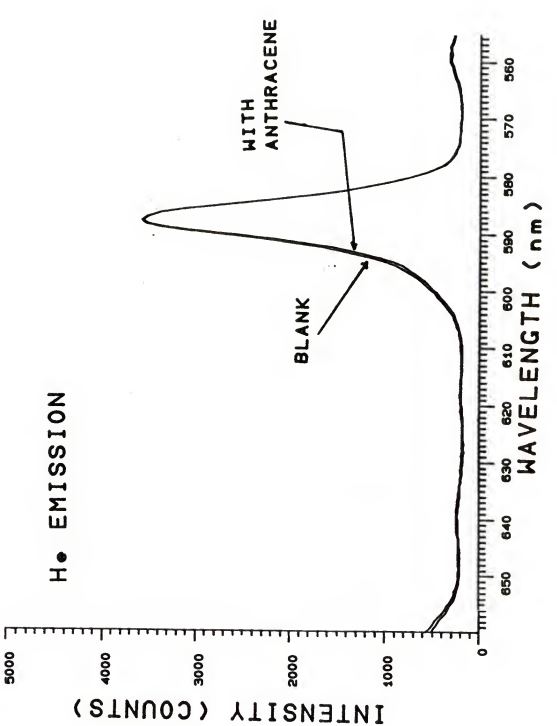
H• EMISSION
INTENSITY (COUNTS)
5000
4000
3000
2000
1000
0
WITH ANTHRACENE
BLANK
650
640
630
620
610
600
590
580
570
560
WAVELENGTH (nm)

in Figure 28. Bandwidths of the He emission of the un-compensated blank and the analyte were also examined for benzo(a)pyrene. The bandwidths at half height and at 10% height, as shown in Figure 29, almost perfectly matched each other.

Both bands will be assumed to be Gaussian functions which can be defined by the mean value and the standard deviation. If the mean value and the standard deviation of one band are equal to that of the other, one of the Gaussian function must be linearly related to the other one. In other words, one band can be matched to the other one by multiplying a constant. In order to calculate the mean value and the standard deviation of the spectral band, the statistical weight of the individual wavelength must be derived first. The straightforward method to obtain this weight is to compute the probability density function, which can be expressed as the following equation:

$$P_i = I_i/\Sigma I_i \tag{3b}$$

where P_i = probability density at wavelength λ_i.

I_i = intensity at wavelength λ_i.

The mean value λ of wavelength is calculated by:

$$\lambda = \Sigma \lambda_i P_i \tag{3c}$$

Finally, the variance of the band can be calculated by the following formula:

$$\sigma^2 = \Sigma(\lambda_i - \lambda)^2 P_i \tag{3d}$$

Figure 28
Helium emission at 585 nm with the presence
of benzo(a)pyrene and the compensated blank.

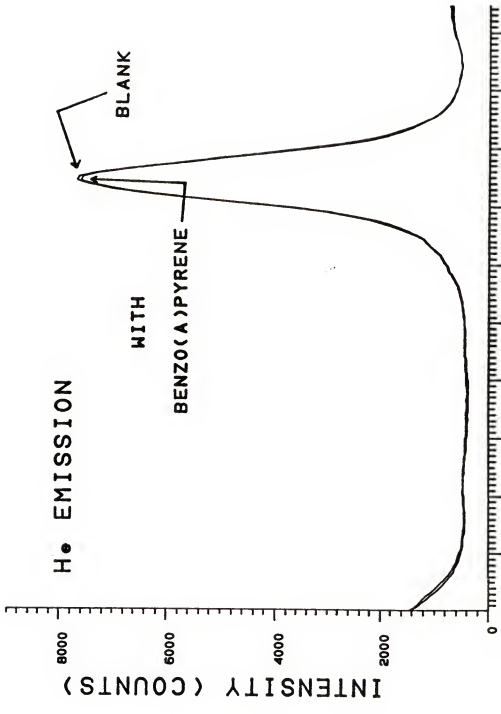
He EMISSION
WITH
BENZO(A)PYRENE
BLANK
INTENSITY (COUNTS)
8000
6000
4000
2000
0
650
640
630
620
610
600
590
580
570
560
WAVELENGTH (nm)

Figure 29
Bandwidths of helium emission at 585 nm with the presence of benzo(a)pyrene and the blank.

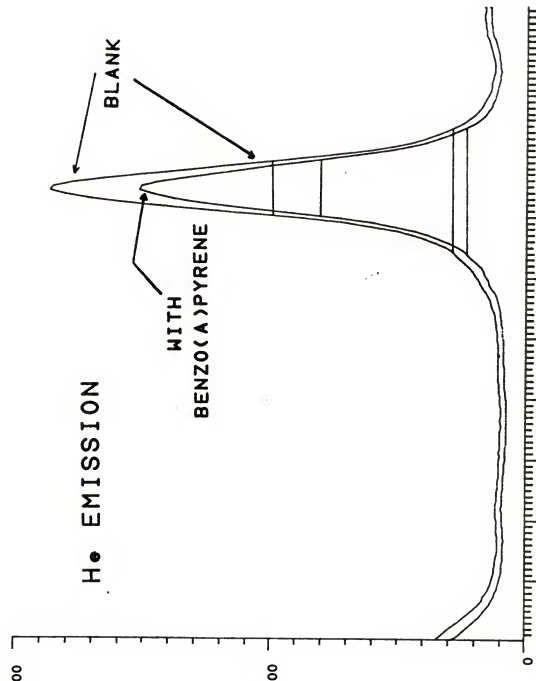
INTENSITY (COUNTS)
10000
5000
0
H• EMISSION
WITH
BENZO(A)PYRENE
BLANK
650
640
630
620
610
600
590
580
570
560
WAVELENGTH (nm)

Thirty one points ranging from 577.9 to 597.7 nm were chosen to cover the peak. The mean value and the standard deviation thus obtained are 587.9 nm and 4.297 nm for the analyte and 588.0 nm and 4.322 nm for the blank, respectively. Apparently, the difference is not very significant.

The emission of the blank was so intense compared with the emission of the analyte that a small perturbation of the He peak intensities could be very significant to the background correction. The intensity of the bumps and troughs is relatively large to those compounds with lower analyte intensity (lower signal-to-noise ratio), such as benzo(e)pyrene, coronene and fluoranthene and is relatively unimportant to those with higher analyte intensity (higher signal-to-noise ratio), such as benzo(k)fluoranthene, perylene and pyrene. Fortunately, the intensity of He emission was lower in the region from 250 to 550 nm where most PAHs luminesce and therefore the background correction error is lower than outside this region.

Quantitative measurement

A scanning monochromator with a photomultiplier tube (PMT) was employed for quantitative measurement. Helium bands detected by the photodiode array (PDA) detector were actually composed of a number of lines which could be resolved with a Heath monochromator in the single channel system; for example, He emission at wavelengths between 390 and 500 nm is shown in Figure 30. To show those lines with lower intensities, the sensitivity of the recorder was adjusted so that several He lines with higher intensities were off-scale.

Figure 30
Helium emission at the wavelengths between 390 and 500 nm with a 100 μm slit width on the Heath monochromator.

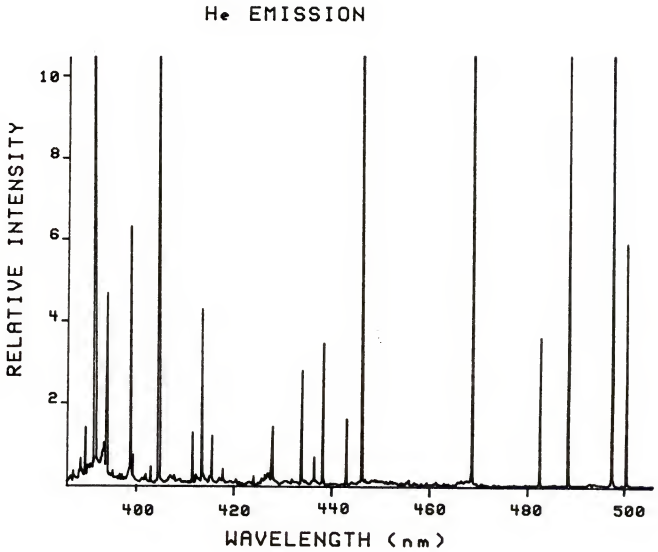
He EMISSION
RELATIVE INTENSITY
10
8
6
4
2
400
420
440
460
480
500
WAVELENGTH (nm)

When 10-20 μL of sample solution in heptane was injected into the empty column, the pressure of the system increased from the initial pressure of about 1 torr to about 10 torr because of the evaporation of the solvent. It took at least 20 s to return to the initial pressure. With the pressure over 5 torr, the plasma was almost extinguished, and no emission from sample was detected under this circumstance. A plasma with a nearly constant pressure was required to obtain reproducible measurements. The large excess of solvent molecules must be removed before taking any measurement. Rather than using a packed GC column, a temperature gradient was applied to separate the analyte from the solvent with the unpacked column.

The solution (PAH in heptane) was injected at 300 ^{o}C into the column at room temperature. Heptane was evaporated under vacuum and pumped out of the system, while the analyte, with a much higher boiling point, presumably condensed and stayed in the column. After the pressure in the system stabilized in about 20 s, the column was heated up at full rate, and the emission of the sample was detected at the peak wavelength (as long as there was no overlapping He emission lines). The column temperature reached 150 ^{o}C in about 2 min. Typical results are shown in Figure 31. The pressure of the system was 1.25 torr with ~ 6 ml min^{-1} He flow. Wavelengths of 445 nm for perylene and 396 nm for pyrene were monitored, with the monochromator slit width set at 250 μm. The measurements were started at the moment when the column was heated up. Amounts of 1 μg of perylene and 2.6 μg of pyrene just provided detectable signals.

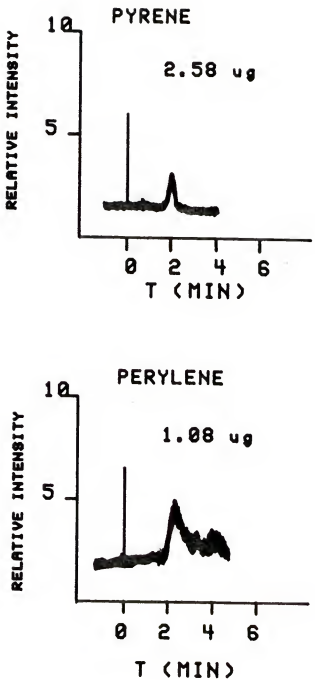

Figure 31
Perylene and pyrene signals at 445 nm and 396 nm
in the electric discharge with a slit width of 250 μm.

Detectable signal of benzo(a)pyrene and fluoranthene was at about the same order of magnitude as perylene and pyrene. Without packing in the GC column, a portion of PAH might have been pumped away with the solvent before the pressure stabilized. The limits of detection were calculated as the amount of analyte estimated to give a signal-to-noise ratio of 3, when the noise was estimated to be one fifth of the peak-to-peak noise on the baseline. The estimated limits of detection for perylene, pyrene, benzo(a)pyrene and fluoranthene are listed in Table V.

Since good sensitivity and limit of detection (~ 0.1 ng) for PAHs was reported by Jurgensen in this laboratory (16), her experimental procedure was therefore carefully followed to examine the results. A sample solution of 1 μL was placed into the test tube which was attached to the alternate sample port, as shown in Figure 2, then the teflon valve was opened for sample introduction. Solvent was evaporated and pumped away very quickly, while the PAH was left on the bottom of the test tube. No signal was ever detected at the emission wavelength for those PAHs. In other words, the previous results were not reproduced. Recently, Yang and Niemzyk have obtained a molecular emission spectrum from intact benzene molecules with an electric discharge system (70). However, they did not report any quantitative data. According to our experimental results, this technique is believed to be impractical for trace analysis.

Table V
Limits of detection for four PAHs

Compound	Wavelength	Limit of Detection (μg)
benzo(a)pyrene	431	1
fluoranthene	475	6
perylene	445	0.2
pyrene	396	0.3

CHAPTER IV
CONCLUSIONS AND FUTURE WORK

Present Work

A study on the afterglow of a reduced pressure nitrogen discharge has been conducted to reevaluate the previously proposed excitation mechanism (16) for benzene and its derivatives. Nitrogen metastable molecules $N_2(A)$ were found to be involved in the excitation of nitric oxide and mercury but not of benzene and anthracene. In addition, helium and argon were also investigated as discharge gases; no luminescence of benzene and anthracene was detected in the afterglow for either gas. It is suggested that the "afterglow" described previously by H. A. Jurgenson in this laboratory is actually part of the primary discharge generated with the concentric glass tubes. In other words, the luminescence of PAHs and other hydrocarbons presumably result from the excitation in the electric discharge instead of with the energy transfer by $N_2(A)$ molecules.

Atomic emission spectrometry with an electric discharge under reduced pressure (glow discharge) has been studied for decades. However, for the first time, luminescence spectra of PAHs were obtained in an electric discharge with the concentric glass tubes; very few physical properties of this electric discharge were previously known. The temperature of the discharge plasma measured in this work was similar to that of a glow discharge. To overcome

the impedance of the dielectric glass wall, a high voltage (> 2.0 kV) was needed to keep the discharge from extinguishing, while only a low voltage (~200 V) is required to sustain a conventional glow discharge once it is started.

Spectra of a number of PAHs were measured. The sensitivity of this technique for PAHs was not good enough for trace analysis. The background radiation of the fill gas was another problem for the broad band molecular spectral analysis.

Future Work

A high vacuum (~10^{-6} torr) electron impact study (71) is suggested for the future work. Sample molecules would be introduced into a vacuum chamber and intercepted by an electron beam which is generated by a heated cathode filament and accelerated by a potential applied to the anode (72). Under high vacuum, collisions of sample molecules with particles other than electrons would be greatly reduced, and the background radiation encountered in the electric discharge would also be minimized. With an increase of the electron beam energy, sample molecules may be broken apart into fragments (73-75). The luminescence of the fragments may also provide potentially useful structural information about the parent molecules (76). The evaluation of the analytical figures of merit would be needed to judge the usefulness of this approach in analytical chemistry.

REFERENCES

1. J. A. Dean and T. C. Rains, "Flame Emission and Atomic Absorption Spectrometry," Marcel Dekker Co., New York (1969).

2. M. Slavin, "Atomic Absorption Spectroscopy," Wiley, New York (1969).

3. C. Th. J. Alkemade and R. Herrmann, "Fundamentals of Analytical Flame Spectroscopy," Adam Hilger Ltd., Britain (1979).

4. S. G. Schulman, "Molecular Luminescence Spectroscopy, Methods and Applications : Part I," Wiley, New York (1985).

5. W. R. Seitz and M. P. Neary, Anal. Chem., 46, 188A (1974).

6. D. G. Sutton, J. E. Melzer and G. A. Capelle, Anal. Chem., 50, 1247 (1978).

7. A. Montaser and D. W. Golinghtly, "Inductively Coupled Plasmas in Analytical Atomic Spectrometry," VCH Publishers, New York (1987).

8. T. M. Sugden and C. N. Kenney, "Microwave Spectroscopy of Gases," D. Van Nostrand Company Ltd., New York (1965).

9. F. K. McTaggart, "Plasma Chemistry in Electric Discharges," Elsevier Publishing Company, New York (1967).

10. S. Caroli, Prog. Analyt. Atom. Spectrosc., 6, 253 (1983).

11. P. F. Little and A. V. Engel, Proc. Roy. Soc., 224A, 209 (1954).

12. D. J. Sturges and H. J. Oskam, J. Appl. Phys., 37, 2405 (1966).

13. H. M. Crosswhite, G. H. Dieke and C. S. Legagneur, J. Opt. Soc. Am., 45, 270 (1955).

14. N. K. Rudnevskii, D. E. Maksimov, T. M. Shabanov and L. P. Lazareva, Zavod. Lab., 38, 1338 (1961).

15. S. Caroli, A. Alimonti and F. Petrucci, Anal. Chim. Acta., 136, 269 (1982).

16. H. A. Jurgensen, Ph.D. dissertation, University of Florida, Gainesville, Florida, (1982).

17. Yu. I. Korovin, Zh. Anal. Khim., 16, 494 (1961).

18. B. A. Tomkins and C. Feldman, Analytica Chimica Acta., 119, 283 (1980).

19. A. N. Wright and C. A. Winkler, "Active Nitrogen", Academic Press, New York, NY (1968).

20. A. P. D'Silva, G. M. Rice and V. A. Fassel, Appl. Spectrosc., 34, 578 (1980).

21. G. W. Rice, J. J. Richard, A. P. D'Silva and V. A. Fassel, Anal. Chem., 53, 1519 (1981).

22. G. W. Rice, J. J. Richard, A. P. D'Silva and V. A. Fassel, J. Assoc. Off. Anal. Chem., 65, 14 (1982).

23. G. W. Rice, A. P. D'Silva and V. A. Fassel, Appl. Spectrosc., 38, 149 (1984).

24. H. C. Na and T. M. Niemczyk, Anal. Chem., 54, 1839 (1982).

25. H. C. Na and T. M. Niemczyk, Anal. Chem., 55, 1240 (1983).

26. W. B. Dodge and R. O. Allen, Anal. Chem., 53, 1279 (1981).

27. J. W. Mitchell, P. K. Wittman and A. M. Williams, Anal. Chem., 58, 371 (1986).

28. P. K. Wittman and J. W. Mitchell, Appl. Spectrosc., 40, 156 (1986).

29. D. G. Sutton, K. R. Westburg and J. E. Melzer, Anal. Chem., 51, 1399 (1979).

30. P. Shubik, Proc. Nat. Acad. Sci. USA, 69, 1052 (1972).

31. H. W. Gerade, "Toxicology and Biochemistry of Aromatic Hydrocarbons," Elsevier, Amsterdam, (1960).

32. D. H. Stedman and D. W. Setser, Chem. Phys. Lett., 2, 542 (1968).

33. F. R. Gilmore, Quant. Spec. Rad. Transfer, 5, 369 (1965).

34. D. H. Stedman and D. W. Setser, J. Chem. Phys., 50, 2256 (1969).

35. D. H. Stedman, J. A. Meyer and D. W. Setser, J. Amer. Chem. Soc., 90, 6856 (1968).

36. D. W. Setser, J. A. Coxon and D. H. Stedman, J. Chem. Phys., 53, 1004 (1970).

37. J. A. Meyer, D. H. Klosterboer and D. W. Setser, J. Chem. Phys., 55, 2084 (1971).

38. J. F. Prince, C. B. Collins and W. W. Robertson, J. Chem. Phys., 40, 2619 (1964).

39. S. Dushman, "Scientific Foundations of Vacuum Technique," 2nd, (J. M. Lafferty ed.), Wiley, New York (1962).

40. W. G. Clark and D. W. Setser, J. Phys. Chem., 84, 2225 (1980).

41. C. B. Collins and W. W. Robertson, J. Chem. Phys., 40, 701 (1964).

42. G. E. Caledonia, S. J. Davis, B. D. Green, L. G. Piper, W. T. Rawlins, G. A. Simons and G. M. Weyl, Report "Analysis of Metastable State Production and Energy Transfer," AFWAL-TR-86-2078, Air Force Wright Aeronautical Labs., USAF, Aeronautical Systems Division (AFSC), Wright Patterson AFB, Ohio.

43. J. Kishman, E. Barish and R. O. Allen, Appl. Spectrosc., 37, 545 (1983).

44. L. S. Ornstein and H. Brinkmann, K. Acad. Amsterdam, 34, 489 (1931).

45. L. S. Ornstein and H. Brinkmann, Physica, 1, 797 (1934).

46. G. F. Kirkbright, M. K. Peters and T. S. West, Talanta, 15, 663 (1968).

47. J. Jarosz, J. M. Mermet and J. P. Robin, Spectrochimica., Acta., 33B, 55 (1978).

48. W. E. Gericke, Z. Astrophysik, 53, 68 (1961).

49. B. S. Malone and W. H. Corcoran, J. Quant. Spectrosc. Radiat., 6, 443 (1966).

50. C. H. Corliss and J. B. Shumaker Jr., J. Res. Nat. Bur. Std., 71A, 575 (1967).

51. W. L. Wiese, Proc. 8th International Conference of Phenomena in Ionized Gases, Vienna, Austria, Springer Verlag, Vienna (1967).

52. B. Wende, Z. Physik, 213, 341 (1968).

53. B. T. Wujec, Acta Phys. Pol., 36, 269 (1969).

54. National Standard Reference Data Series, National Bureau of Standard 4, Atomic Transition Probablities (1966).

55. P. Shubik, Proc. Natl. Acad. Sci. USA, 69, 1052 (1972).

56. E. L. Wynder and K. Mabuchi, Prev. Med., 1, 300 (1972).

57. G. Nagata, M. Kodama, and Y. Ioki, "Polycyclic Hydrocarbons and Cancer" (H. V. Gelboin and P. O. P. Ts'o eds.), P 247, Academic Press, New York, (1978).

58. M. L. Lee, M. V. Novotny and K. D. Bartle, "Analytical Chemistry of Polycyclic Aromatic Compounds," Academic Press, (1981).

59. A. P. Ilnitsky, G. A. Belitsky and L. M. Shabad, Cancer Lett. (Amsterdam), 1, 291 (1976).

60. A. P. Ilnitsky, G. A. Belitsky and L. M. Shabad, Cancer Lett. (Amsterdam), 3, 227 (1977).

61. M. Blumer and W. W. Youngblood, Science, 188, 53 (1975).

62. B. D. Crittenden and R. Long "Carcinogenesis-A Comprehensive Survey" (R. I. Frendenthal and P. W. Jones, eds.) Vol I, P 209, Raven, New York (1976).

63. M. L. Lee, M. Novotny and K. D. Bartle, Anal. Chem., 48, 405 (1976).

64. S. Y. Su, Ph.D. Dissertation, University of Florida, Gainesville, Florida (1982).

65. E. P. C. Lai, Ph.D. Dissertation, University of Florida, Gainesville, Florida (1982).

66. M. J. Kerkhoff, Ph.D. Dissertation, University of Florida, Gainesville, Florida (1984).

67. G. R. Kornblum and L. de Galen, Spectrochim. Acta., 32B, 71 (1977).

68. D. M. Mehs and T. M. Niemczyk, Appl. Spectrosc., 35, 66 (1981).

69. A. R. Striganov and N. S. Sventitskii, "Tables of Spectral Lines of Neutral and Ionized Atoms," Plenum, New York (1969).

70. J. T. Clay and T. M. Niemczyk, Spectroscopy, 2, 36 (1987).

71. M. L. Robin, G. K. Schweitzer and E. L. Wehry, Appl. Spectrosc. Review, 17, 165 (1981).

72. T. Ogawa, I. Fujita, M. Hatada and K. Hirota, Bull. Chem. Soc. Jpn., 44, 659 (1971).

73. C. I. M. Beenakker and F. J. DeHeer, Chem. Phys. Lett., 29, 89 (1974).

74. C. I. M. Beenakker and F. J. DeHeer and L. J. Dosterhoff, Chem. Phys. Lett., 28, 320 (1974).

75. C. I. M. Beenakker and F. J. DeHeer and L. J. Dosterhoff, Chem. Phys. Lett., 28, 320 (1974).

76. C. A. Gierczak, M. A. Heindorf and J. Allison, Anal. Chem., 56, 2966 (1984).

BIOGRAPHICAL SKETCH

Tiing Yu was born on August 27, 1954 in Tainan, Taiwan, Republic of China. He obtained his B.S. in chemistry in 1976 from the National Cheng Kung University of Taiwan. After working and wandering for many years, he found his way to graduate school at the University of Florida where he met and married to Pei-Chen in May 1987. They did not know each other in Taiwan but travelled half the globe to Florida, USA.

I certify that I have read this study and that in my opinion it conforms to acceptable standards of scholarly presentation and is fully adequate, in scope and quality, as a dissertation for the degree of Doctor of Philosophy.

James D. Winefordner, Chairman
Graduate Research Professor of Chemistry

I certify that I have read this study and that in my opinion it conforms to acceptable standards of scholarly presentation and is fully adequate, in scope and quality, as a dissertation for the degree of Doctor of Philosophy.

Stephen G. Schulman
Professor of Pharmaceutics

I certify that I have read this study and that in my opinion it conforms to acceptable standards of scholarly presentation and is fully adequate, in scope and quality, as a dissertation for the degree of Doctor of Philosophy.

Richard A. Yost
Associate Professor of Chemistry

This dissertation was submitted to the Graduate Faculty of the Department of Chemistry in the College of Liberal Arts and Sciences and to the Graduate School and was accepted as partial fulfillment of the requirements for the degre of Doctor of Philosophy.

December 1987

Dean, Graduate School